AN ABSTRACT OF THE THESIS OF

Elizabeth Ruth Tucker for the degree of Master of Science

in Geology presented on August 14, 1975

Title: GEOLOGY AND STRUCTURE OF THE BROTHERS FAULT ZONE IN THE CENTRAL PART OF THE MILLICAN SE QUADRANGLE, DESCHUTES COUNTY, OREGON

Redacted for privacy

Abstract approved: _____
Dr. Robert Lawrence

The thesis is a structural and petrographic study of approximately 23 square miles in the Millican SE quadrangle, Deschutes County, Oregon. The area lies along the Brothers fault zone.

Bedrock in the area is of Pliocene to Recent age and consists of an older basaltic unit with an associated dacite, a younger dacite, and a younger basaltic unit. The older basaltic unit and both dacites have been severely faulted. The younger basaltic unit has filled in topographic lows and is relatively undeformed.

The dominant faults in the area are en echelon high-angle normal faults trending N. 40°W. with vertical displacements up to 600 feet. Cross faults with smaller displacements trend N. 45°E. The normal faults are Reidel and conjugate Reidel shears and are interpreted as the surface expression of a deep-seated right lateral displacement. The fault zone displaces units of Miocene to Pleistocene age and is considered to have been active during that time.

Geology and Structure of the Brothers Fault Zone in the Central Part of the Millican SE Quadrangle, Deschutes County, Oregon

by

Elizabeth Ruth Tucker

A THESIS

submitted to

Oregon State University

in partial fulfillment of
the requirements for the
degree of

Master of Science

Commencement June 1976

APPROVED:

Redacted for privacy

Assistant Professor of Geology
in charge of major

Redacted for privacy

Chairman of the Department of Geology

Redacted for privacy

Dean of Graduate School

Date thesis is presented August 14, 1975

Typed by Opal Grossnicklaus for Elizabeth Ruth Tucker

ACKNOWLEDGMENTS

Greatest appreciation and thanks are extended to Dr. Robert Lawrence who suggested the thesis problem and followed me all the way through it. He gave generously of his time and knowledge.

Both Dr. Edward Taylor and Dr. Harold Enlows critically read the manuscript and offered suggestions. In addition, Dr. Taylor with the assistance of Ms. Ruth Lightfoot performed the chemical analyses.

Appreciation is extended to Ken Spitze for providing the computer program used in calculating the stress-strain curves.

Various people helped me in the preparation of the manuscript. George Kendall critically read the draft copy. Harry Grimmnitz drafted Plate III. Nancy Mears provided much needed moral support.

Special thanks are extended to Omar and Betty Moffitt and Pam and Ron Moffitt, the residents of the thesis area, who often had me to dinner, provided water, fixed my car, and generally kept an eye on me.

TABLE OF CONTENTS

LIST OF FIGURES

LIST OF PLATES

GEOLOGY AND STRUCTURE OF THE BROTHERS FAULT ZONE IN THE CENTRAL PART OF THE MILLIGAN SE QUADRANGLE, DESCHUTES COUNTY, OREGON

INTRODUCTION

Purpose

The main objectives of the thesis have been to construct a detailed geologic map of a segment of the Brothers fault zone and to describe the lithologic units encountered. The location of the thesis area was chosen because there are several lithologically distinct units present which permit a study of the relative age of faulting.

In addition, a structural map of the Brothers fault zone was constructed and the structural development of the fault zone described in detail. The structural development of the thesis area has been related to the Brothers fault zone as a whole.

Location and Accessibility

The mapped area is in the central part of the Millican SE quadrangle. It can be reached by driving thirty five miles east of Bend on Highway 20, then six miles south on Con Gurney Road to its intersection with Fox Butte and Moffit Roads. The mapped area covers portions of T. 20S., R. 16E., and T. 21S., R. 16E. (Fig. 1).

All of the mapped area is within two miles of gravel roads or

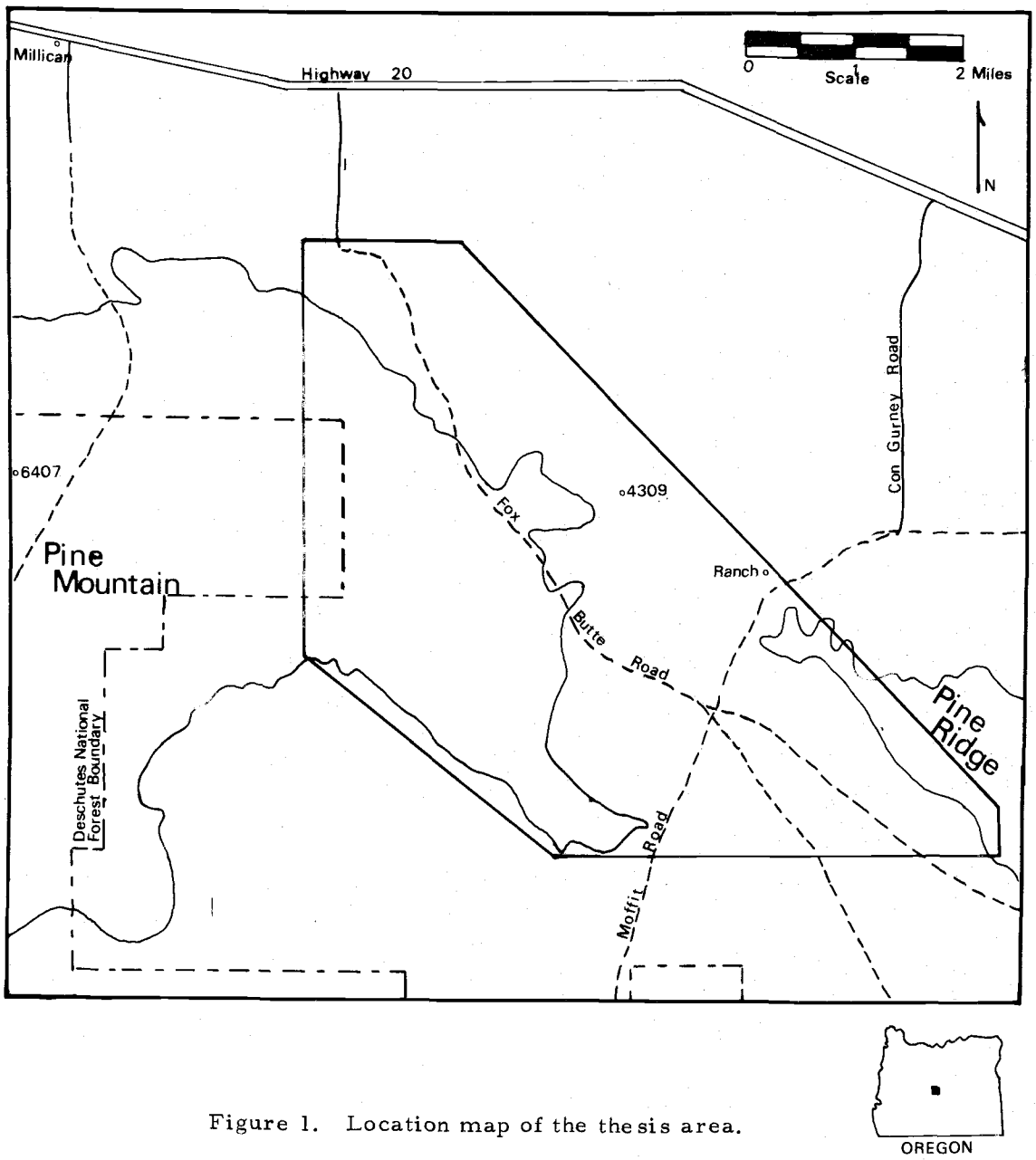

Figure 1. Location map of the thesis area.

jeep trails and is easily reached by foot. The topography is typical of the High Lava Plains Province and the elevation ranges from 4000 to 6000 feet. Bedrock is exposed in approximately 25% of the mapped area. Excellent exposures occur along tops of ridges and in gullies; scattered exposures occur throughout the rest of the area. The Moffitt Ranch is an active cattle ranch just inside the east boundary of the thesis area and is the only local source of water.

Methods of Investigation

Field work was carried out during June, July, and August of 1974. The base map is the 7 1/2' Millican SE quadrangle Oregon. Aerial photos with a scale of 1:24,000 were used to aid in the mapping. A Brunton compass was used to take attitudes.

Samples collected in the field were used for several laboratory studies. Selected samples were studied in thin section with a petrographic microscope. Plagioclase composition was determined by a combination of the Michel-Levy statistical method and the combined Carlsbad-albite twin method. Vesicle fillings and aeolian deposits were studied with the aid of a binocular microscope.

Whole rock chemical analyses were performed by Dr. Edward M. Taylor and Ms. Ruth Lightfoot of the OSU Geology Department, X-ray fluorescence spectrometry (FeO, CaO, K_2O, TiO_2), atomic absorption spectrophotometry (MgO, Na_2O), and the colorimetric

method of visible light spectrophotometry (SiO_2) were used. All iron is recorded as FeO. The determination of H_2O is not available.

Triaxial deformation experiments were carried out on a Donath 30,000 P. S. I. triaxial deformation apparatus. The data were compiled and transformed to stress-strain curves by the Oregon State University CDC 3300 computer.

The volcanic rocks are classified petrographically according to Williams, Turner, and Gilbert (1964) and chemically according to the following divisions based on weight percent of SiO_2; basalt, less than 52% SiO_2; basaltic andesite, 52 to 58% SiO_2; andesite, 58 to 66% SiO_2; dacite, 66 to 74% SiO_2; rhyolite, greater than 74% SiO_2 (after Taylor, personal communication). Rock colors are based on the "Rock Color Chart" (Goddard and others, 1963).

GEOLOGIC SETTING

Regional Tectonics

The thesis area straddles the Brothers fault zone near Bend, Oregon. The fault zone extends N. 75°W. from Steens Mountain to Bend and consists of en echelon faults, none of which is more than 12 miles long. The Brothers fault zone separates the Basin and Range Province, an area of recent east-west extension to the south, from the mountains of north central Oregon, an area of little east-west deformation during the same time interval (Lawrence, in press).

During the Pliocene the fault zone provided vents for large volumes of volcanic material forming the flows of the High Lava Plains Province (Fig. 2). This province is bounded on the north by the Blue Mountains Province, on the west by the Cascade Range Province, and on the south by the Basin and Range Province (Baldwin, 1964).

Regional and Local Geology

The volcanic material of the High Lava Plains Province is predominantly basalt with a high alumina trend and associated rhyolites, dacites, and pyroclastics. The high-alumina basalts form one of three groups of late Cenozoic basalts in the Pacific Northwest as described by Waters (1962). The second group is made up of the

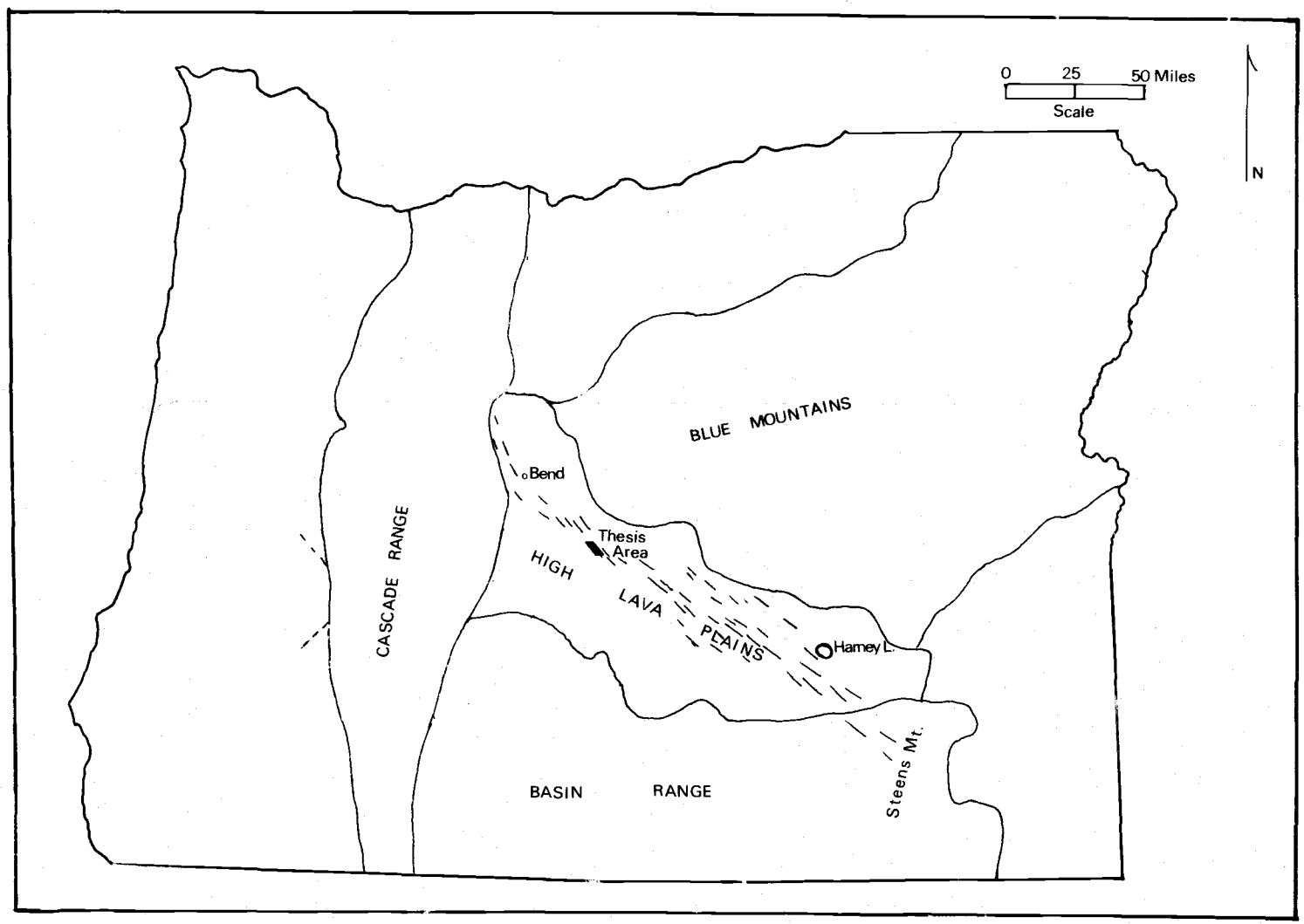

Figure 2. Location of the High Lava Plains Province (after Baldwin, 1964, p. 4).

Columbia River tholeiitic basalt of Miocene to lower Pliocene age. The Columbia River basalt is present over a wide area in eastern Oregon and Washington and northwestern Idaho and extends an unknown distance south under the High Lava Plains Province. The area of Columbia River basalt south of Prineville is the nearest outcrop to the study area (Fig. 3). The Cascade Range hypersthene andesite volcanics and high-alumina basalts form the third group and occur west of the High Lava Plains Province (Fig. 3). They are Pliocene to Quaternary in age.

Volcanic sedimentary rocks (tuffaceous sandstones, siltstones, and conglomerates) and lacustrine deposits are interbedded with basalt flows of the High Lava Plains Province. Alluvium, playa lake deposits, fan deposits, and aeolian deposits of sand, ash, and pumice cover low areas throughout the province.

The thesis area lies east of Pine Mountain, a silicic dome with a complex of rhyolitic to dacitic flows. A very young (Quaternary) basalt lies in a broad flat plain east of the area. Tuffaceous lacustrine deposits are found in a basin north of the area and are visible in road cuts along Highway 20. A late olivine basalt mapped in the thesis area extends south where it is covered by more recent cinder cones and associated lava flows (Fig. 4).

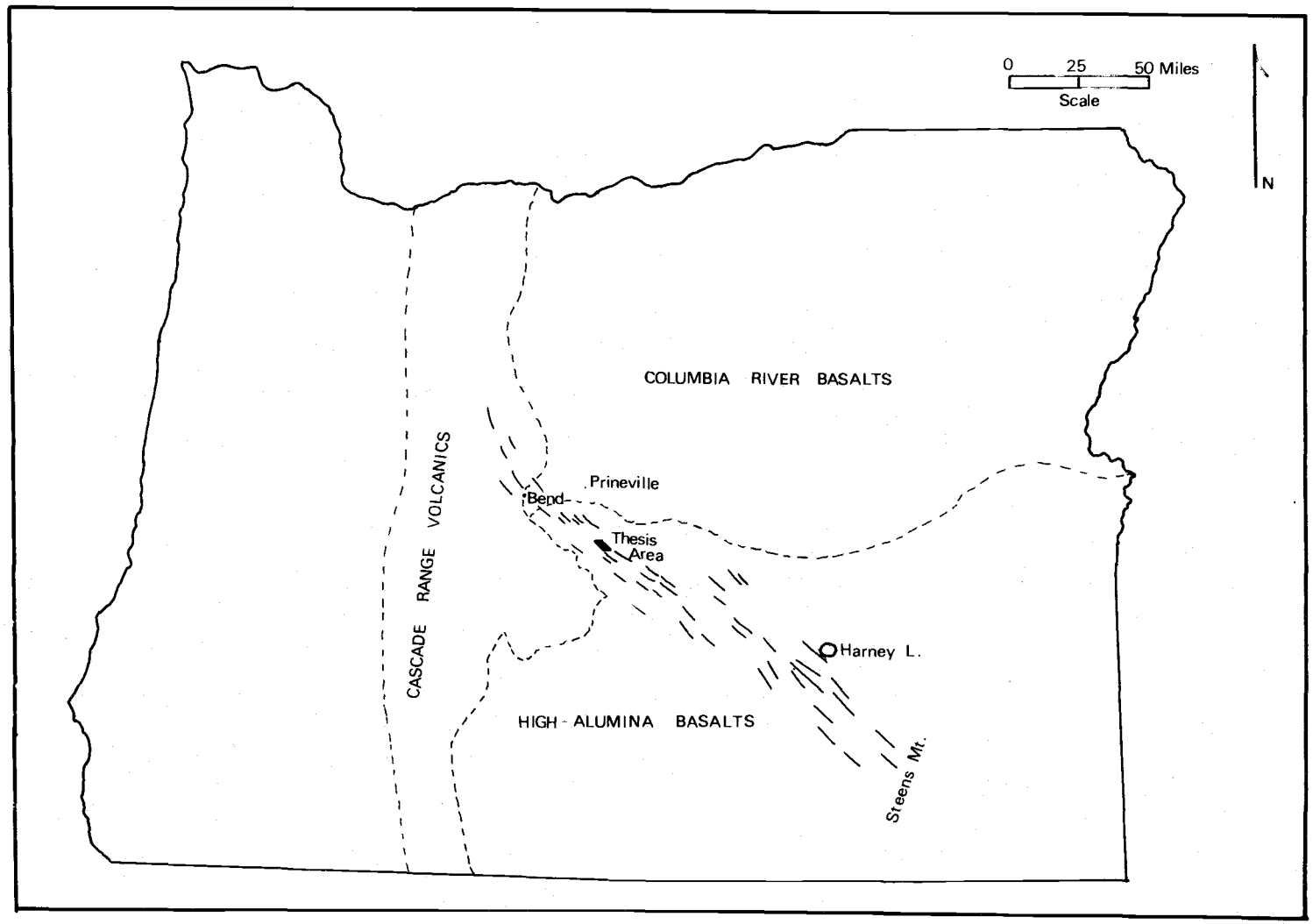

Figure 3. Three groups of late Cenozoic basalts in Oregon (after Waters, 1962, p. 159).

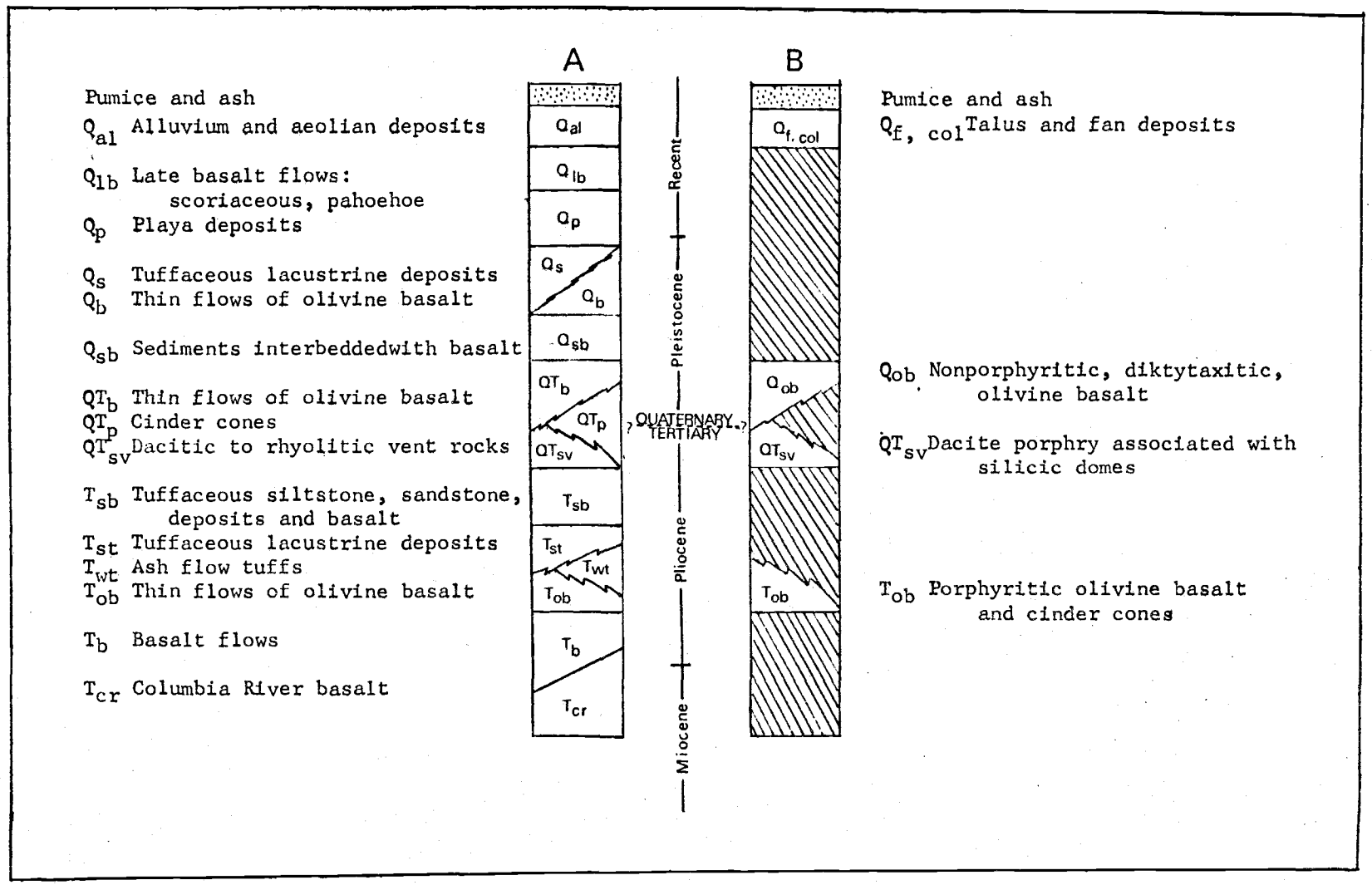

Figure 4. A. Regional stratigraphic column (after Walker and others, 1967).
B. Associated units of the thesis area.

Previous Investigations

The thesis area lies in the eastern half of the Crescent 1:250,000 quadrangle which was reconnaissance mapped by photogeologic and field methods (Walker, Peterson, and Greene, 1967). Higgins and Waters (1967), Walker (1969, 1974), and Lawrence (in press) all discussed the Brothers fault zone. Ages of silicic volcanic rocks of central Oregon were published by Walker (1974) and ages of basaltic rocks were published by Walker, Dalrymple, and Lanphere (1974). Waters (1962) described the high-alumina basalts of the High Lava Plains and Higgins (1969) described the airfall ash and pumice lapilli deposits from Newberry Caldera which blanket the thesis area.

STRATIGRAPHY

General Statement

Bedrock in the mapped area consists of two widespread basaltic units and two little exposed units of dacite (Fig. 4). The two basaltic units have been distinguished on the basis of microscopic petrography, structure, and geomorphology. The two basaltic units are informally termed the "older basaltic unit" and the "younger basaltic unit," herein. The more elevated, faulted, and topographically irregular areas are underlain by the older basaltic unit. The younger basaltic unit fills in the low areas, is relatively undeformed, and shows relict surficial flow structures.

The dacites are distinguished on the basis of location and lithology. The older of the two dacites is intimately associated with the older basaltic unit and makes up the prominent hill known locally as The Brothers. The younger dacite occurs in the west side of the area and is part of the Pine Mountain silicic dome complex.

The units show a distinct bimodal distribution in composition typical of the Basin and Range Province. There are no rocks intermediate in composition. Chemical analyses (Appendix 1) indicate a tholeiitic trend for the basaltic units based on a graph by MacDonald and Katsura (1964).

Older Basaltic Unit

The older basaltic unit is the oldest unit exposed in the thesis area. It is found on the ridges in the east and west sides of the area and also covers the north central part of the area. The basaltic unit varies in outcrop expression and texture. Two main types are distinguished on the basis of texture: a porphyritic olivine basalt or basaltic andesite and a fine-grained olivine-bearing basaltic andesite.

Field Description

The total thickness of the older basaltic unit was not determined but is at least 650 feet. Individual lava flows are thin; the largest flow observed is 30 feet thick indicating that at least 25 flows are present. The flows were not mapped individually because they are not laterally continuous and are highly faulted. Instead they have been separated into a coarse-grained member and a fine-grained member based on the above textural differences.

Most of the older basaltic unit (approximately 75% of the exposed unit) consists of the coarse-grained member. Phenocrysts of plagioclase and olivine are visible in a coarse to medium-grained (one to two mm), medium to light gray (N 5 to N 7) groundmass. Outcrop expression varies from massive to scoriaceous, the vesicles of the latter being one to ten mm in diameter. Many

vesicles are stretched (Fig. 5) and "cross-bedded" due to flow (Fig. 6) and some are filled with chalcedony and calcite. The basalt weathers to a rusty brown (10 R 5/4). Outcrops exhibit spheroidal weathering (Fig. 7) and some weathered surfaces have a polygonal pattern which may be the result of cooling (Fig. 8).

The flows of the coarse-grained member are four to thirty feet thick. The thicker flows vary in appearance from bottom to top and can be divided into three parts. The bottom part of a thick flow is platey (Fig. 9). The plates are one to twelve inches thick, are not laterally continuous, and grade upward into more massive (structureless) basaltic material. The plates cannot be used to determine flow direction or amount of tilting because they do not necessarily parallel the base of the flow. Some of the larger sections of the plates are curved (Fig. 10). Massive basaltic material forms the central part of a thick flow (Fig. 11). The weathered surfaces are smooth. The top part or surface of a thick flow is formed of blocks of basaltic material one to five feet in diameter (Fig. 12). These lie in semi-random orientation on the underlying massive part. Vesicles occur in this part of the flow.

The thinner flows of the coarse-grained member of the older basaltic unit consist of large blocks approximately three to four feet in diameter which are similar to the top part of the thick flows.

Approximately 25% of the older basaltic unit is fine-grained

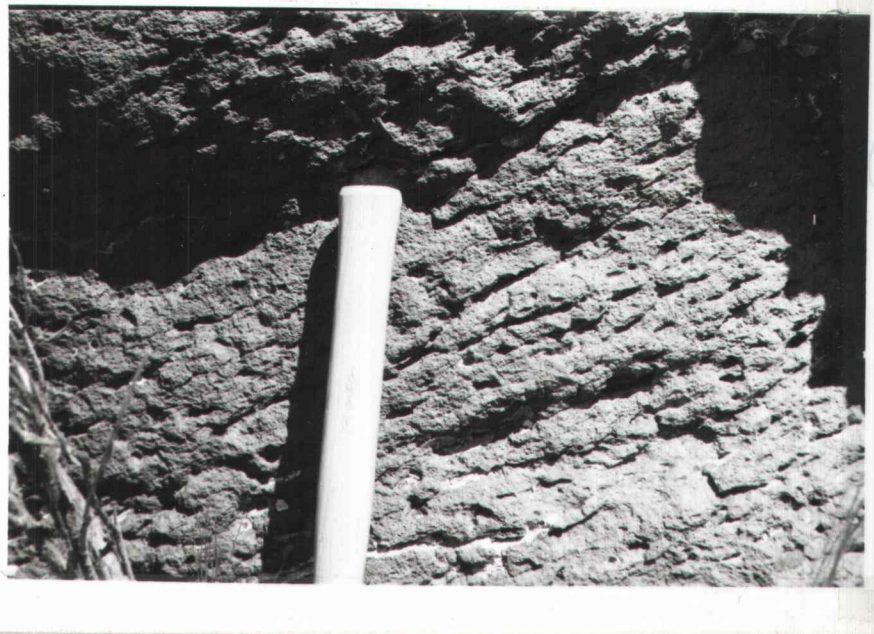

Figure 5. Stretched vesicles in an older basaltic unit flow.

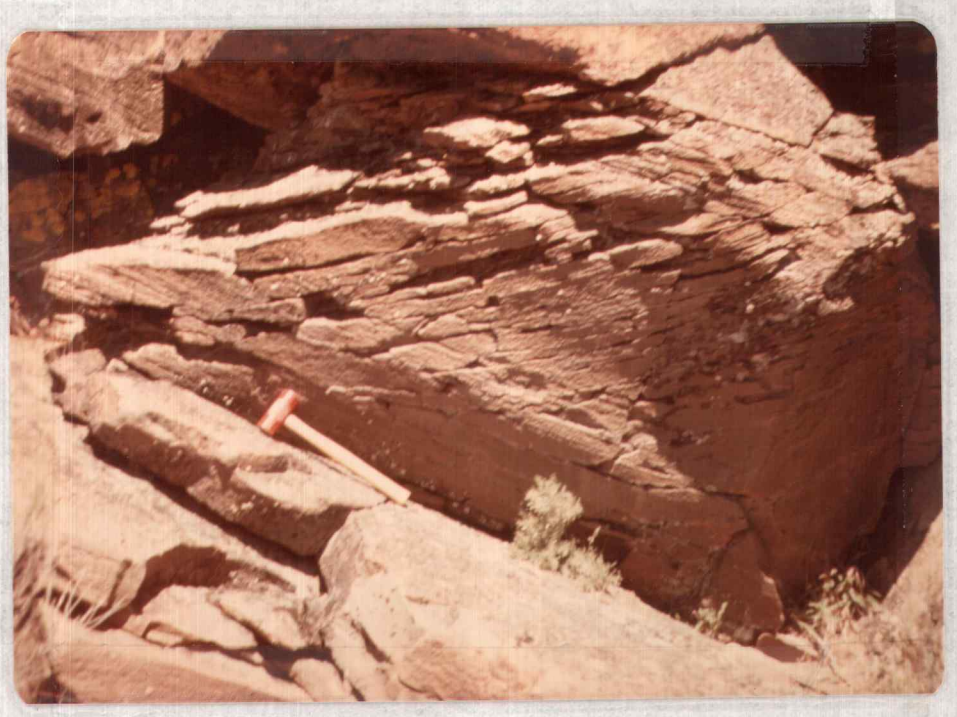

Figure 6. "Crossbedded" stretched vesicles in an older basaltic unit flow.

Figure 7. Spheroidal weathering in the older basaltic unit.

Figure 8. "Polygonal pattern" on the weathered surface of an older basaltic flow.

Figure 9. The bottom part of a thick flow showing platey structure.

Figure 10. A thick flow of the older basaltic unit showing a curved platey section.

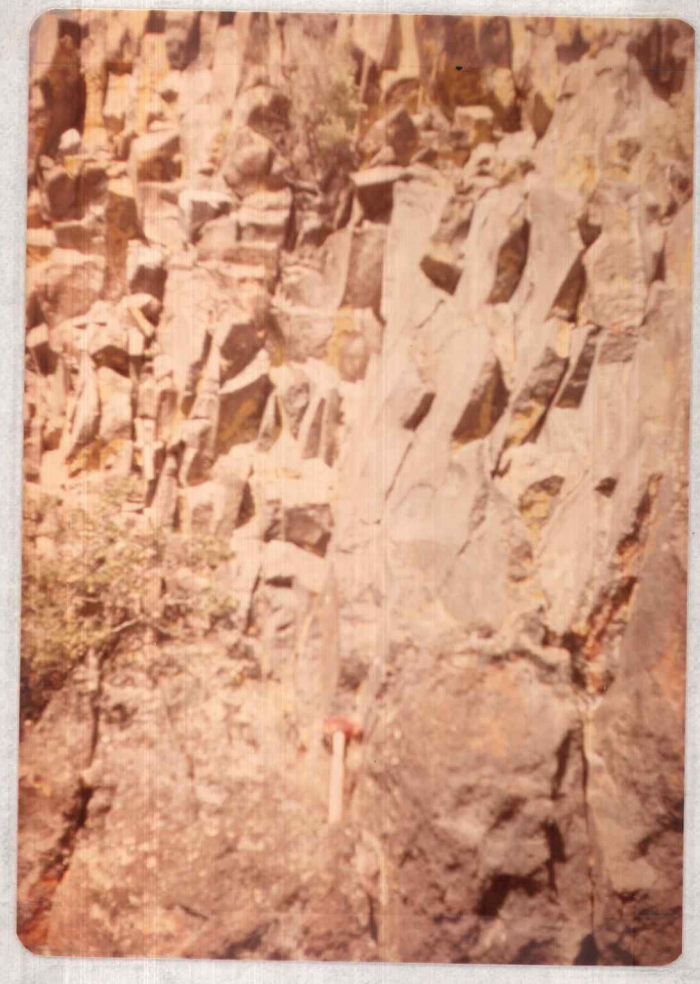

Figure 11. The central part of a thick flow showing massive structure.

Figure 12. The top part of a thick flow showing semi-random orientation of basaltic blocks.

(less than one mm), dense to vesicular, black to medium gray (N 1 to N 5) basaltic andesite. This rock type is found chiefly in the northern part of the area, but similar flows are present in the southern part where these flows occur interbedded with more typical coarse-grained flows described above. The flows are a maximum of 15 feet thick. The rock is massive to blocky in outcrop. Some surfaces are spheroidally weathered; others are irregular and knobby. The rock weathers to a rusty brown (10 R 5/4).

Two cinder cones are located in the southern part of the area. They are 1/4 mile in diameter and deeply eroded so that the central plugs are exposed (Fig. 13). A less eroded cinder cone is located in the center of the mapped area (Sec. 10, Plate I). The highest part of the northeast ridge (Sec. 17, Plate I) is another possible location of a cinder cone. The cones are associated with layers of red basaltic flows and large amounts of cinder. The cinder cones are probably vents for some of the flows of the older basaltic unit; they are intimately related to the older basaltic flows. Reddish basaltic flows interbedded with scoriaceous debris dip away from the centers of the cones and grade into the typical flows of the older basaltic unit (Fig. 14). Occasional small units of red, massive to scoriaceous basaltic flow rock, accompanied by cinders, occur elsewhere in the older basaltic unit; but no structures indicative of cinder cones are associated with them. These red units are

Figure 13. Deeply eroded cinder cone.

Figure 14. Reddish basaltic flows dipping away from probable vent on a hill in Sec. 20 (Plate I).

probably oxidized basaltic lava formed within scoriaceous flow surfaces.

A dike cuts across part of the older basaltic unit in the southern part of the thesis area. The dike is similar in composition to the basaltic unit it cuts. It has a chilled margin and was probably a conduit for a late flow of the older basaltic unit. The dike occurs near a cinder cone and must have formed close to the surface on which the cinder cone developed. The later flows formed by the dike have been eroded away.

Petrography

The coarse-grained member of the older basaltic unit is holocrystalline. It contains numerous phenocrysts and glomerocrysts (Fig. 15) of plagioclase, olivine, and some augite in a groundmass of plagioclase, olivine, augite, and magnetite. The phenocrysts form ten to thirty percent of the rock and are one to two mm in length. The glomerocrysts are two to three mm in diameter. The groundmass of some flows exhibits a pilotaxitic texture due to alignment of the small laths of plagioclase (Fig. 16).

A large flow in sections 5 and 6 (Plate I) in the southern part of the thesis area is vitrophyric (Fig. 17). Olivine and plagioclase phenocrysts two mm long occur in a glassy matrix which shows some flow banding. This flow is related in age to the older basaltic

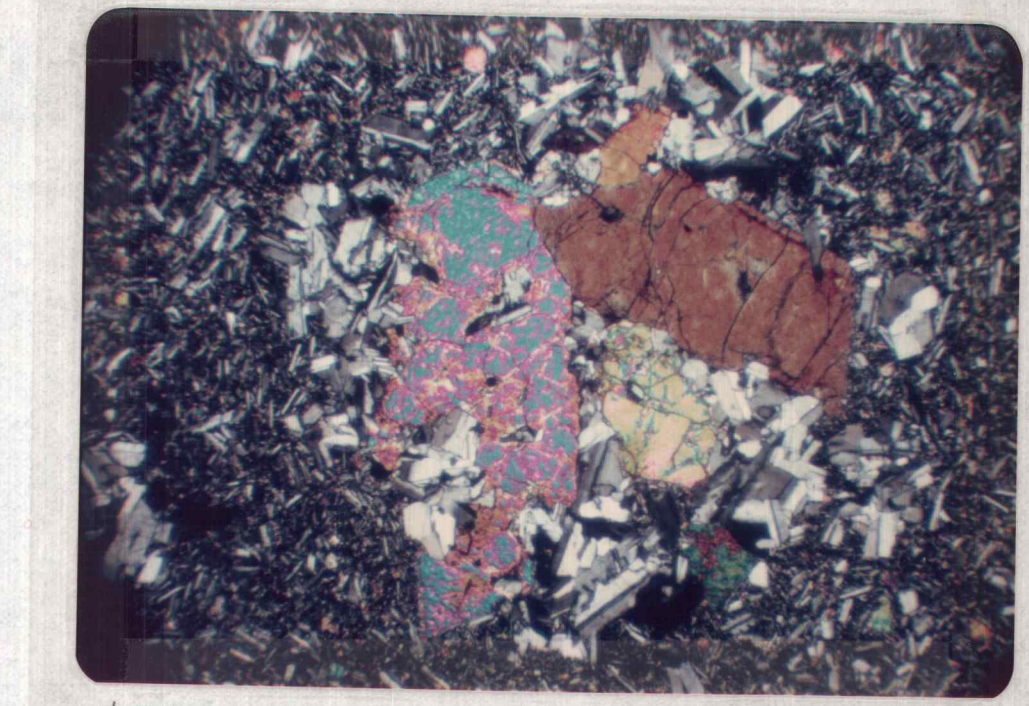

Figure 15. Glomerocryst of olivine and plagioclase in the coarse-grained member of the older basaltic unit. Crossed nicols.

Figure 16. Pilotaxitic texture of the older basaltic unit. Crossed nicols.

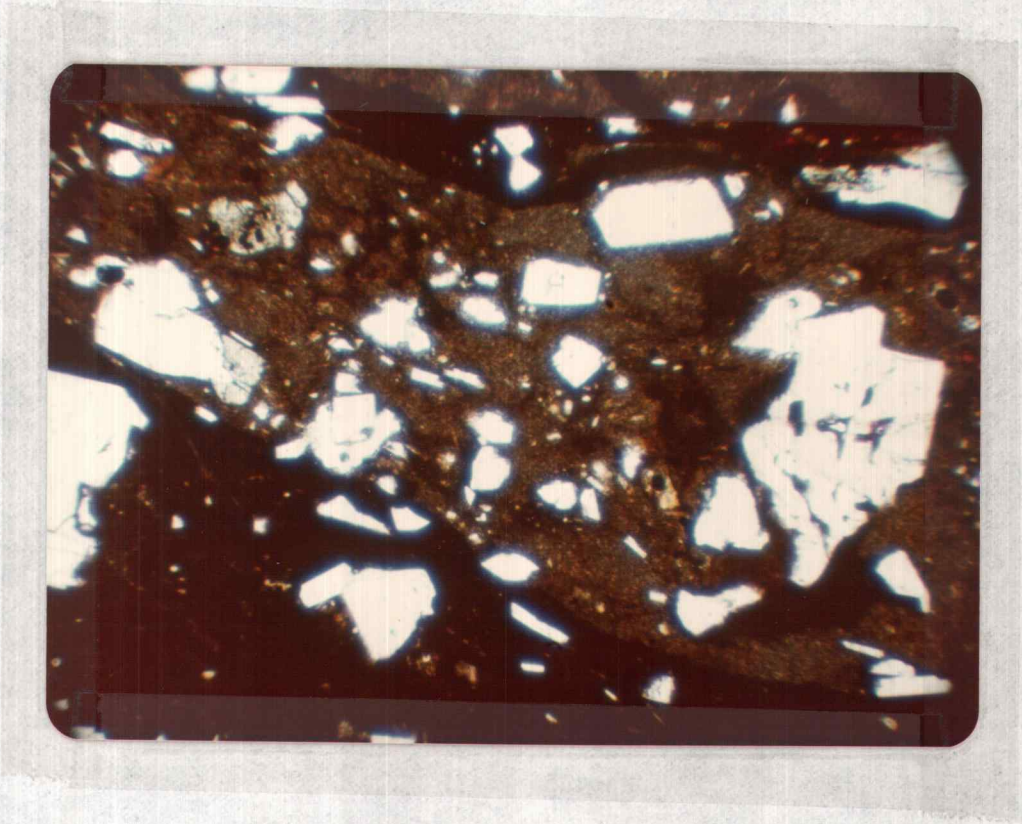

1 mm

Figure 17. Vitrophyric flow of the older basaltic unit. Phenocrysts of plagioclase and olivine in a silicic matrix. Uncrossed nicols.

unit but is more silicic than the rest of the older unit. Because of its local occurrence and distinct difference in composition, it is not included in the following petrographic discussion.

The fine-grained member of the older basaltic unit is hypocrystalline. It contains crystals less than 1/2 mm in length of plagioclase, augite, olivine, and magnetite with interstitial glass. The glass comprises only three to five percent of the rock.

The mineralogy of the two types of the older basaltic unit is quite similar. The following discussion of the minerals pertains to both types except where specified.

Plagioclase phenocrysts are abundant forming 15 to 30% of the rock. The compositions range from An_{55} to An_{65}. Oscillatory zoning with a normal trend is prevalent (Fig. 18). The phenocrysts are generally euhedral, however the largest crystals are irregular in shape and contain inclusions of magnetite, glass, and possibly other minerals (Fig. 19). The phenocrysts have good crystal outlines but many are embayed. The olivine in the groundmass occurs as small anhedral grains.

Augite occurs only rarely as phenocrysts but is common in the groundmass and forms as much as 14% of the rock. It is often subophitic, partially enclosing small plagioclase laths (Fig. 20). It has an extinction angle of 40 to 50° and a 2V of about 50°. Hypersthene was found in the groundmass of only one fine-grained flow sampled.

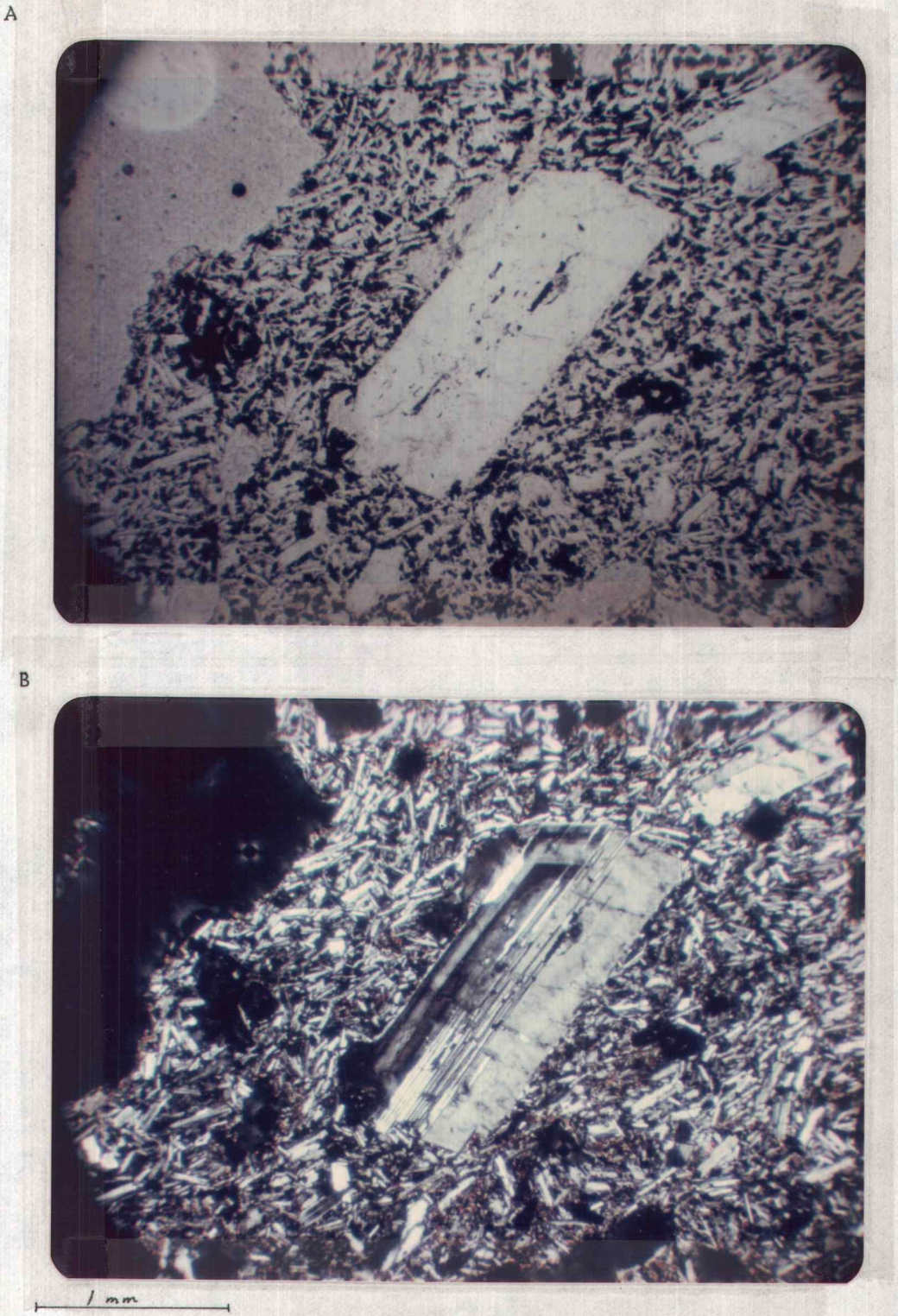

Figure 18. A. Plagioclase phenocryst in the coarse-grained member of the older basaltic unit. Uncrossed nicols.

B. The same plagioclase phenocryst under crossed nicols showing oscillatory zoning.

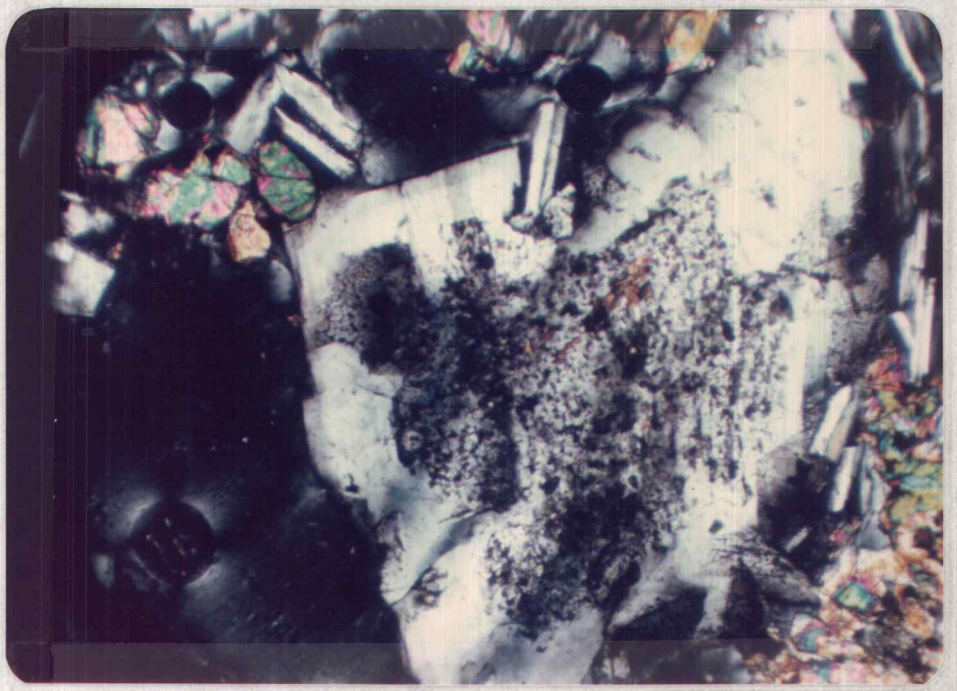

Figure 19. Magnetite and glass inclusions in a plagioclase phenocryst. Crossed nicols.

Figure 20. Subophitic augite in the older basaltic unit. Crossed nicols.

Magnetite is an abundant accessory forming one to three percent of the rock. In several of the very coarse flows primary magnetite is up to one mm in diameter. In general it occurs as small grains in the groundmass. Secondary magnetite forms as an alteration product of the olivine.

Apatite is a very minor constituent forming less than 1/2% of the rock. It occurs as very fine needles in the groundmass of the coarsest flows.

Younger Basaltic Unit

The younger basaltic unit, a diktytaxitic medium-grained (one to two mm) olivine basalt, is the youngest volcanic unit in the thesis area. It consists of a series of thin, blocky flows filling the low-lying parts of the area. The probable source of the lava is to the south, an area which is covered by younger basaltic flows so that the actual vents are obscured. The lava flowed north filling the basin in the southeastern part of the area and continued down a canyon to the northeast (Sec. 27 Plate I).

Field Description

The younger basaltic unit has low relief. Outcrops are visible in stream gullies (Fig. 21) and along pressure ridges. The flows are approximately ten feet thick with a lower massive part and an

upper blocky part. Surface flow features such as pressure ridges and tumulae exist, but inner flow features are not visible. There are a few blocky outcrops with vesicles. Fresh surfaces are medium dark gray (N 4); weathered surfaces are dark gray (N 3) to black (N 1). The younger basaltic unit is distinguished from the older basaltic unit by its consistent equigranular and diktytaxitic texture and by its topographic position, though it was often difficult to separate the fine-grained member of the older basaltic unit from the younger basaltic unit.

Petrography

The younger basalt is diktytaxitic and fine to medium-grained (Fig. 22). Large phenocrysts are rare but ten percent of the rock is formed of plagioclase and olivine crystals slightly larger than the groundmass.

Plagioclase forms 90% of the rock and occurs as well formed laths less than 1/2 mm in length. Crystals exhibit both simple and laminar twinning. The composition of the plagioclase ranges from An_{58} to An_{63}. Rare irregular phenocrysts of plagioclase greater than 1/2 mm long contain glassy blebs and inclusions of magnetite. The rims of these crystals, though embayed, are clear.

Olivine forms one to three percent of the rock and occurs as subhedral to anhedral crystals altered slightly to iddingsite. The

Figure 21. The younger basaltic unit is exposed in the lowest visible outcrop which was cut by a gully.

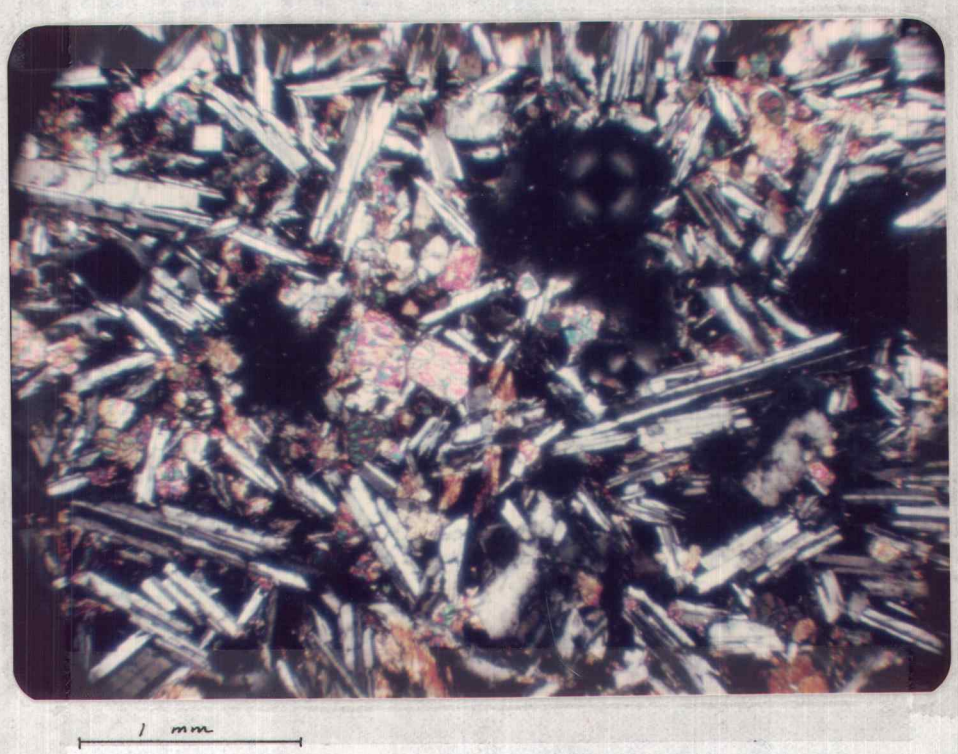

Figure 22. The diktytaxitic younger basaltic unit. Crossed nicols.

The olivine is forsteritic with a 2V close to 80°.

Augite occurs mainly in a subhedral crystalline form but also in a semi-fibrous form. The crystalline augite is subophitic. Augite forms one to three percent of the rock.

Magnetite occurs as an accessory. Its primary form is as small anhedral grains. It occurs also as a secondary mineral after the alteration of olivine.

Dacites

There are two distinct dacites present in the thesis area. They differ in outcrop expression, in mineralogy, and in apparent age relationship to the basalts. They are described separately below.

Older Dacite

The older dacite occurs in the eastern part of the area. It forms the part of Pine Ridge locally referred to as The Brothers. The dacite is younger than the older basaltic unit but has undergone the same amount of deformation. It is younger than the older basaltic unit because it intrudes the older basaltic flows along Pine Ridge. However, it is older than the main episode of faulting and, therefore, the younger basalt.

The dacite is well weathered. Fresh surfaces are light gray to white (N 7 to N 9). Weathered surfaces are dark gray (N 3) to

pale reddish brown (10 R 5/4). Fresh samples are hard to obtain since outcrops are brittle and fractured. The fracture planes are nearly vertical and strike approximately northeast-southwest.

The rock is an olivine-bearing prophyritic dacite (70% SiO_2, see Appendix I). Euhedral to subhedral phenocrysts of plagioclase form approximately 15% of the rock. Both simple and laminar twinning are present. The phenocrysts are normally zoned with an average composition of An_{48}.

Olivine xenocrysts form three to four percent of the rock. They show strong resorption textures and are altered to iddingsite and magnetite (Fig. 23). They were probably removed from the edges of the magma conduit and carried along in the magma.

Magnetite also occurs as a primary mineral. Less than one percent of the rock is formed of subhedral magnetite grains.

The light gray groundmass of the dacite forms 80% of the rock and is extremely fine-grained to glassy. Poorly outlined plagioclase microlites show a trachytic texture.

Younger Dacite

The younger dacite is associated with the Pine Mountain complex. It forms a steep-sided, symmetrically shaped hill in the west side of the thesis area (Fig. 24). The younger dacite has been faulted along the southeast flank of Pine Mountain but has not been

1/4 mm

Figure 23. Xenocryst of olivine and plagioclase phenocrysts in the older dacite. Uncrossed nicols.

faulted to the north and east. The dacite covers the faulted older basaltic unit and is, therefore, younger than the older basaltic unit.

The younger dacite is a porphyritic hypersthene-bearing dacite (73% SiO_2, see Appendix I). It is grayish pink (5 R 8/2) to light gray N 7) on fresh surfaces and weathers to a medium gray (N 5). Outcrops are platey but there are no visible flow structures.

Euhedral to subhedral phenocrysts of plagioclase form 12 to 14% of the rock. These are approximately 1/2 mm in length and exhibit simple and laminar twinning. Some of the phenocrysts show extreme oscillatory zoning suggesting a change in melt composition. The average composition of the phenocrysts is An_{55}.

Subhedral phenocrysts vary from 1/3 to 1/2 mm in length and form three percent of the rock (Fig. 25). They are pleochroic in shades of light green, pink, and yellow. The 2V is high, indicating an iron content of 70%.

Large opaque oxides (magnetite) up to 1/2 mm long form two percent of the rock and are alteration products of hornblende. There is less than one percent unaltered hornblende preserved.

Magnetite also occurs as a primary mineral. Grains of magnetite in the groundmass form one percent of the rock.

The groundmass is extremely fine-grained and trachytic. It forms 80% of the rock and is made up of plagioclase, oxides, and a light green mineral (pyroxene?).

Figure 24. Steep-sided, symmetrically shaped hill or dome formed by the flows of the younger dacite.

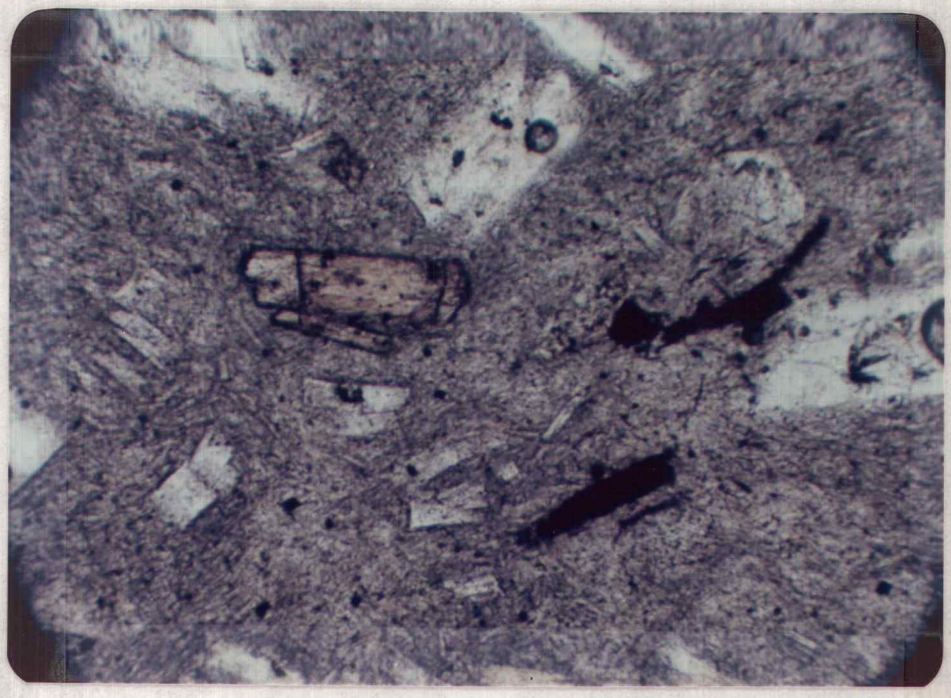

Figure 25. Hypersthene (pink), hornblende altered to magnetite (black), and plagioclase (white) phenocrysts in the younger dacite. Uncrossed nicols.

Surface Deposits and Geomorphology

A partial record of Recent volcanic activity in the High Lava Plains Province is contained in the regolith of the thesis area. The regolith is found everywhere in the area and consists of poorly bedded, unconsolidated, volcaniclastic debris. Exposures are poor because of the blanket-like nature of the deposit; the maximum thickness is estimated at 15 feet. The unit is thickest in topographic lows, where both pumice lapilli and ash are abundant, and thinnest on highs where pumice lapilli are abundant. Individual beds vary in thickness from one to five inches. The beds are difficult to distinguish and vary primarily in content and size of cinder and pumice. The grains of the deposit are angular and poorly sorted; grains range from ash size to 20 mm lapilli. The unit consists primarily of cinders, pumice, and ash; but lithic fragments, plagioclase, magnetite, and olivine are also present.

The distribution and horizontal bedding of the regolith imply aeolian deposition. Some of the volcanic debris may have had its source in a group of cinder cones approximately ten to fifteen miles to the south of the thesis area. Activity there has been dated at one half to one million years ago (Walker, 1974). Ash from the eruption of Mt. Mazama was not identified.

A one to five cm thick bed of pumice lapilli forms the uppermost

continuous layer of the regolith. The pumice is found throughout the thesis area with few exceptions: steep east-facing slopes have very little or no pumice. The pumice is thickest on west-facing slopes. The pumice ranges in size from one to twenty mm and is white to buff in color. Some of it is tinted red by the soil.

The source of this deposit was the Central Pumice Cone of the Newberry Caldera (Higgins, 1969). During the second eruption of the pumice cone, ungraded pumice lapilli and ash were transported by strong west-northwest winds and deposited as far as 40 miles east of the caldera. The pumice decreases in size from west to east. Close to the caldera the pumice is as large as seven cm in diameter. The eruption has been dated at 1720±250 years ago (Higgins, 1969).

Overyling the Newberry ash on the south side of the Pine Mountain ridge are thin (six to twelve inches thick) aeolian deposits of fine-grained, very light gray sand. The deposits are irregular in shape, up to 50 yards across, and are found on the windward side of the mountain. The sand is very well sorted and angular to subrounded. Grains consist of plagioclase, olivine, magnetite, and pyroxene crystals, and pumice, obsidian, and lithic fragments. Plagioclase is the most abundant constituent and explains the light color of the sand. The sand has been winnowed out from deposits to the southwest of the thesis area, carried across Kotzman Basin, and deposited on the ridge.

Thin alluvial fan deposits occur in the northern part of the thesis area at the base of one drainage basin and in the eastern part of the thesis area at the base of another drainage basin. The fans consist mostly of sand and silt, are of low relief, and are locally farmed. The geomorphology of the area is controlled by the structure. The drainage pattern takes the form of the fault pattern; stream gullies are formed along faults. One major stream gully diverges from this pattern; it follows the contact between the older basaltic unit and the younger basaltic unit in the eastern part of the thesis area.

Two of the major faults have very steep scarps which are covered with talus. The talus obscures the outcrop and the stratigraphy is unknown.

The outcrops of hard rock which face southwest have long parallel grooves one to five mm deep. The major storm winds blow north-northeast and have polished and grooved the rocks with pumice and sand (Fig. 26).

Sequence of Events

The geologic history of the thesis area essentially begins in the late Tertiary period. The pre-Pliocene history has been obscured by the Pliocene to Recent flows.

Figure 26. Grooves cut and polished by pumice and sand blasting.

The older basaltic unit, the oldest unit visible in the thesis area, has been correlated with other basalts and basaltic andesites of Pliocene age (Walker and others, 1967). The thin parallel flows suggest that they were extruded on a surface with low relief. Some source vents lie in the area. The horizontal flows of the older basaltic unit are abruptly truncated along the southeast margin of the area by the older dacite which intruded the older basaltic unit during this period. The main period of faulting began following the extrusion of the older basaltic unit and older dacite.

The younger dacite, related to Pine Mountain (for which a date is not yet available), was extruded near the end of the period of faulting. A main fault cuts the dacite in the southwestern part of the area. Shortly after this, the extrusion of the younger basaltic unit filled the low sections of the area. The flows remain undeformed except for one normal offset in the eastern part of the area. The younger basaltic unit unconformably overlies the older basaltic unit and the older dacite.

The deposition of wind-borne ash and pumice lapilli followed the last extrusion. Little erosion has taken place and the rock units and faults are well preserved.

STRUCTURE

General Statement

The Brothers fault zone extends from Steens Mountain to Bend, Oregon and is a relatively young feature along which the faults are well preserved and distinct. Two sets of faults, designated herein as "main" and "cross" faults, have been formed in the zone. The thesis area lies in the northwest portion of the zone and was chosen because the two sets of faults are well developed there and because there are several chronologically distinct units which provide information on the age of faulting. The faults in the thesis area were studied in detail by the author by field work and on aerial photographs in order to compare the structure of the thesis area with that of the rest of the fault zone.

Local Structure

The general trend of the Brothers fault zone through the thesis area is N. 50°W. The thesis area spans the fault zone, and the two classes of faults, main and cross faults, are the primary local structures. The main faults strike N. 45°W. at angles of 5° to 20° to the fault zone and the cross faults strike N. 40°W. to N. 55°W. at angles of 80 to 85° to the main faults. Deformation in the thesis area is the result of faulting. The lava flows have behaved in a brittle manner

and have been tilted and broken with localized zones of crushed rock. There has been no folding.

Topographic expression of the faults in the area is excellent. The main faults are distinguished in the field as distinct scarps which show little wasting on their dip slopes, but which are covered with abundant talus at the base of their scarps. The cross faults are largely expressed as stream gullies. The main faults show the greatest vertical displacement and tilt the once horizontal lava flows of the older basaltic unit as much as 15°. The main faults are all steeply dipping ones, the majority of which are more than three miles long. The gullies that identify the cross faults are the result of streams flowing down the main tilt blocks and localized in zones of crushed rock. Most of the cross faults are less than a mile long with the exception of a two mile long cross fault near the center of the area. The presence of the cross faults along the gullies is confirmed by changes in lithology across the faults, abrupt termination of some of the main faults, and the presence of zones of disrupted rock.

Quantitative estimates of displacements of the faults are difficult to determine because the displaced lava flows are thin and discontinuous. There are no useful marker beds. However, minimal estimates for the displacements along the main faults are possible at several localities because there has been little post-faulting

erosion of the fault scarps. Relief along the flank of Pine Mountain above Kotzman Basin in the southwest part of the area suggests a minimum of 550 to 600 feet of vertical offset. The elevation of Pine Ridge in the eastern part of the area is 550 to 600 feet above the basin to its west and 800 feet above the basin to its east. These are minimum estimates because the basins have been filled with an undetermined thickness of the younger basaltic unit. Other main faults show lesser elevation differences but most have displacements over 50 feet. More than 1000 feet of displacement may be present on some.

The degree of offset on the main faults decreases away from the center of the fault zone. Figure 27 shows successive cross-sections of a main fault with decreasing amount of offset from the center of the fault zone. This main fault eventually disappears under the unfaulted younger basaltic flows.

Displacements on the cross faults are much smaller. The maximum appears on the two mile cross fault where there is an apparent downdrop of 40 feet on the south side of the fault. Most cross faults have less than 20 feet of offset.

The main faults produce an almost uniform set of east tilted fault blocks. All but two of the fault planes are on the west side of the fault blocks and dip to the west. Lava flows in the blocks dip from 15° east at Pine Ridge to 2° east in a block (Sec. 26, Plate I)

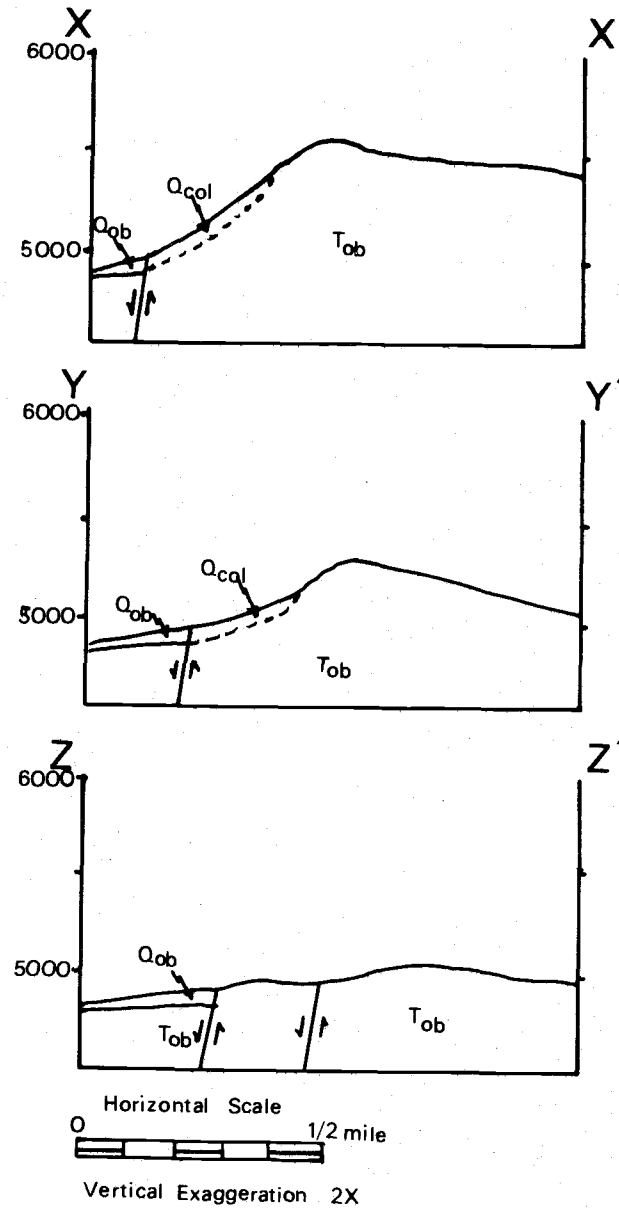

Figure 27. Successive cross-sections of a main fault showing the decrease in offset as the fault gets farther from the center of the fault zone.

with very low relief. In general, the blocks with greater offset have greater rotation. Attitudes estimated on the Pine Mountain and Pine Ridge faults suggest that the fault planes are steeply dipping, 75 to 80° west, in the area. (See cross-sections, Plate II). One exception to this general picture is a fault plane which dips steeply to the east in the central portion of the area (Cross-section BB', Plate II) with a graben now filled with colluvium to its east. A hinge fault in the central portion of the area is another exception to the general structural pattern. The hinge appears to be in the area of the long cross fault. North of the cross fault the main fault is uplifted on the east side and the block produced tilts eight degrees to the east. To the south of the cross fault the main fault is uplifted on the west side and the fault block produced is a horst with a westward dipping fault on its west side.

The relative sequence and age of the faulting is well established in the area though the absolute ages are not known. The wide distribution and planar flow layering of the older basaltic unit suggests low relief in the thesis area prior to its eruption. This indicates that the current Brothers fault zone has developed in the thesis area since this event. The faults displace the older basaltic unit and older dacite. The younger dacite covers some cross faults but is displaced by other main faults. The younger basaltic unit filling in the low area is largely unfaulted. The one exception is a main fault in the

eastern part of the thesis area. Thus, the younger basaltic unit postdates the main period of faulting. The cross faults are offset by the main faults and appear to have formed just before or simultaneously with the main faults.

Regional Structure

The Brothers fault zone consists of a group of en echelon faults trending N. 50°W. across central Oregon (Fig. 1). The en echelon or main faults are from one to twelve miles long. Cross faults at approximate angles of 80° to the main faults are less than one mile long and occur only in portions of the zone. The east end of the zone is at Steens Mountain and the western end runs into and becomes part of the Sisters trend (Lawrence, in press). To the north, the faulting gives way to folding in the Blue Mountains. To the south the en echelon faults curve into faults of the Basin and Range. Examples of this gradation can be seen in the vicinity of Wagontire (Plate III).

The Brothers fault zone was mapped using U-2 hi-flight photos with a scale of 1:120,000. The photos were taken from NASA flights 72-114 and 74-110a. The faults were transferred to the Adel, Bend, Burns, and Crescent 1:250,000 quadrangles (Plate III). All structural lineaments observed on the ground surface were mapped as faults. The hi-flight photos did not cover an approximately eight mile wide strip running east-west across the zone. These faults were filled in

by direct use of maps by Walker, Peterson, and Greene (1967) and Greene, Walker, and Corcoran (1972).

In general, the faults appear to be steeply dipping normal faults. The apparent vertical offset for some faults is a minimum of 600 feet as observed in the thesis area. Other faults have smaller displacements. Where possible the upthrown sides of the faults are marked on Plate III. Some cinder cones appear to have minor lateral as well as vertical offset. If lateral offset is present elsewhere, it is not visible due to the lack of well formed drainage patterns and varying lithologic units. The fault zone has been divided into three sections for discussion on the basis of changes in the trend of the zone and in the appearance of the fault pattern.

A section of the fault zone trends N. 50°W. from Steens Mountain to Glass Butte and consists of main faults two to twelve miles long which strike approximately N. 40°W. There are no cross faults except in the area west of Harney Lake. There the main faults are concentrated and a few cross faults are apparent which strike N. 25°E. Wave cut cliffs and beach lines in the vicinity of Harney Lake may be confused with faults, but most parallel the trend of the faults and their general direction is probably fault controlled. Few faults show up in the area west of Wagontire and was probably eroded by the headwaters of Wilson Creek. The main faults between Steens Mountain and Glass Butte are longer and farther apart than those in

the thesis area, and there are fewer cross faults. This section ends just north of Glass Butte.

Another section of the zone begins just south of Glass Butte and swings slightly west to Pine Mountain. At Hampton the fault zone trends N. 58°W. and at Brothers its trend has changed to N. 70° W. The main faults at Hampton are two to ten miles long and strike N. 45°W. At Brothers the faults become shorter, two to six miles long, and strike N. 60°W. The main faults in this entire section are numerous and closely spaced, and cross faults are abundant. The area south of Brothers was checked on a brief reconnaissance. In comparison with the thesis area, the fault planes are more steeply dipping but show less vertical offset (Fig. 28). The faults are well defined by unweathered scarps and the low areas have not been filled by a younger basaltic unit.

The last section begins at Pine Mountain and the thesis area and trends N. 50°W. until the fault zone swings north at Black Butte to become part of the Sisters Trend. The thesis area is different from the rest of the section. Its main faults are three to six miles long striking N. 45°W to N. 35°W. and cross faults are abundant. To the northwest of the thesis area, the cross faults die out, and the main faults become longer, six to twelve miles long, and strike N. 35°W. The northwest section is similar to the section between Steens Mountain and Glass Butte.

A.

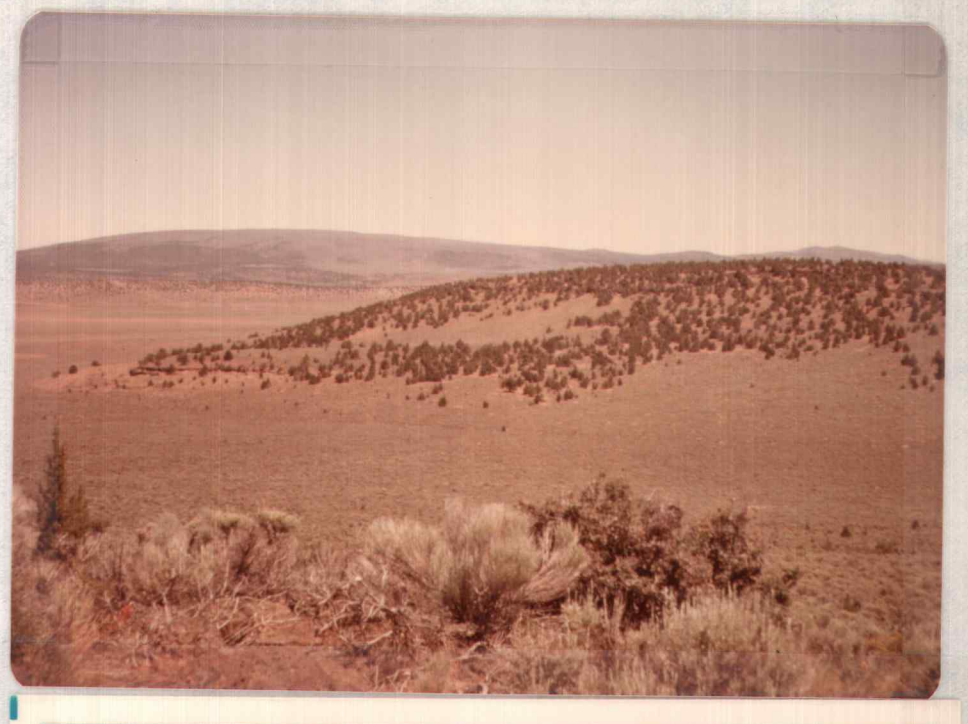

B.

Figure 28. A comparison of the faults in the thesis area with those in the area south of Brothers.

A. Faults in the thesis area have great vertical displacement. The fault planes dip 70 to 75°.

B. Faults in the area south of Brothers have lesser displacements. The fault planes are nearly vertical forming abrupt scarps.

The approximate age of faulting has been correlated with the age of volcanic activity (Walker, 1974), as the latter is thought to be the result of tectonic disturbances. The units visible at the surface along the fault zone are basalt flows, rhyolitic domes, ash-flow tuffs, and related volcaniclastic sedimentary rocks. The units are Miocene to Recent and show a decrease in age from southeast to northwest. The basalts (dates from Walker and others, 1974) show a very general decrease in age from Steens Mountain (fifteen million years) to an area just north of the thesis area (six to seven million years). Silicic domes (Walker, 1974) show a marked decrease in age from Duck Butte (ten million years) to China Hat (0.76 million years). This would indicate that faulting began at Steens Mountain approximately fifteen million years ago and slowly migrated northwest. The last stages of active faulting were ten million years ago in the vicinity of Steens Mountain and activity ended at a later time farther northwest along the fault zone.

The units of the thesis area do not correspond with this general picture. The older basaltic unit of the thesis area is correlated with the six to seven million year old basaltic flow north of Millican as mapped by Walker and others (1967, 1974). The older basaltic unit erupted before the main stage of faulting instead of resulting from the faulting and the six million year date may be too old for the onset of tectonic activity in the thesis area. The younger basaltic

unit of the thesis area has not been faulted and it postdates the main stage of faulting, but it is covered by the volcanic material of China Hat. Therefore, the age of 0.76 million years for the final stage of faulting in the thesis area may be too young. A date for the silicic complex of Pine Mountain is needed because it more likely correlates with the last stages of faulting in the thesis area.

Stewart, Walker, and Kleinhampl (1975) have included the Brothers fault zone in the Oregon-Nevada lineament, a term they have suggested for a 750 km long northwest trending belt of en echelon faults from central Nevada to central Oregon. They attribute this belt to a single fracture system or to a series of strike-slip and tension zones and suggest this as a possible alternative model to the development of the Brothers fault zone as a distinct and separate feature.

TECTONIC INTERPRETATION

The Brothers fault zone is a striking feature of regional northwest tectonics and is especially interesting because it separates an area of extension from an area of relative compression (Lawrence, in press). The extensional faults of the Basin and Range are thought to result from brittle fracture of surface rocks in response to plastic extension of the substratum (Stewart, 1971). This produces a particular geometric fracture pattern which is related to the state of stress at failure (Donath, 1962). The Brothers fault zone has a consistent pattern of main faults and cross faults which correlate with a strike-slip fault pattern produced by Tchalenko (1970) in his Reidel experiment.

Structural Model

A study of shear zone structures was undertaken by Tchalenko (1970) in which he compared structures formed in the Reidel experiment with structures found in fault zones on a regional scale. The Reidel experiment consists of placing several millimeters of clay paste over two adjacent horizontal boards. One board is moved slowly past the other and the clay is deformed as the board moves. Five stages have been defined in the deformation process. The first is the peak strength stage in which Reidel shears are formed at

angles of 12° to the line of displacement between the boards and then are rotated as far as 16° to this line. When clays with low water content are used, shears called conjugate Reidel shears are formed at angles of 78° to the line of shear during this stage. The second stage is a post peak strength stage during which the Reidel shears rotate closer to the shear line and new Reidel shears may form at angles of eight degrees to the shear line. The third is also a post peak strength stage during which "P shears," faults symmetrical to the Reidel shears with respect to the line of shear, develop. The pre-residual strength stage is the fourth stage during which continuous horizontal shears are developed. The last stage is the residual strength stage in which a single displacement shear forms parallel to the shear line and is the prominent feature.

The fault pattern of the thesis area is as well developed as any portion of the Brothers fault zone and, therefore, is representative of the structure of all portions of the fault zone. The main faults in the thesis area are formed at 5 to 20° to the trend of the fault zone and can be correlated with the Reidel shears of the first deformation stage which formed at angles of 12 to 16° to the line of shear. The cross faults in the thesis area formed at angles of 90 to 105° to the main trend of the fault zone. These can be correlated with the conjugate Reidel shears produced at angles of 78° to the line of shear in the experiment. The differences in angles can be attributed to the

inhomogeneity of the rocks in the thesis area and the uncontrolled conditions during the period of faulting. In the experiment, the conjugate Reidel shears are formed just before or simultaneously with the formation of the Reidel shears and this relationship was noted between the main and cross faults in the field.

The general pattern of the faults in the thesis area can be correlated with the pattern of faulting produced during the peak strength stage of the Dasht-e Bayaz earthquake of 1968 (Tchalenko and Ambraseys, 1970). However, faults produced there were strike-slip faults with little vertical displacement and the faults in the thesis area are normal faults with no discernible lateral displacement. A simple paper model (Fig. 29) of right lateral strike-slip motion shows that if the ends of the developing Reidel shears are stationary instead of allowing their opposing sides to move past one another, normal faults with little lateral displacement are produced. This is one way to account for the development of normal faults in the Brothers fault zone.

The structural features of the thesis area described above indicate that the fault pattern of the thesis area correlates with the pattern produced by the first stage of deformation in the Reidel experiment. According to this model, the thesis area is underlain by a deep-seated right lateral strike-slip fault which has reached the peak shear strength of deformation. The fault zone is right lateral because

A.

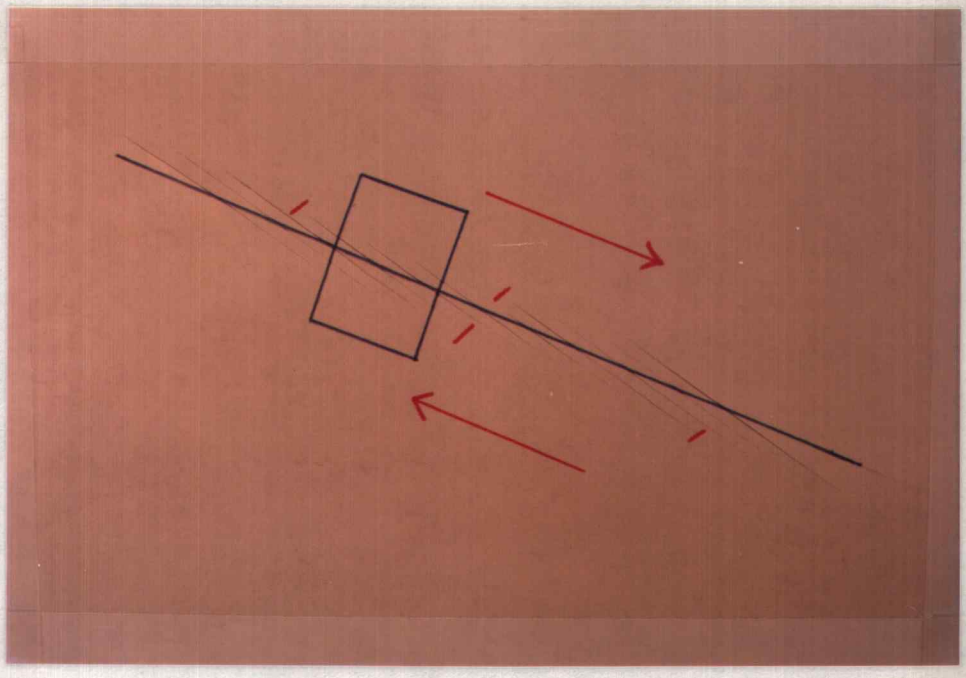

B.

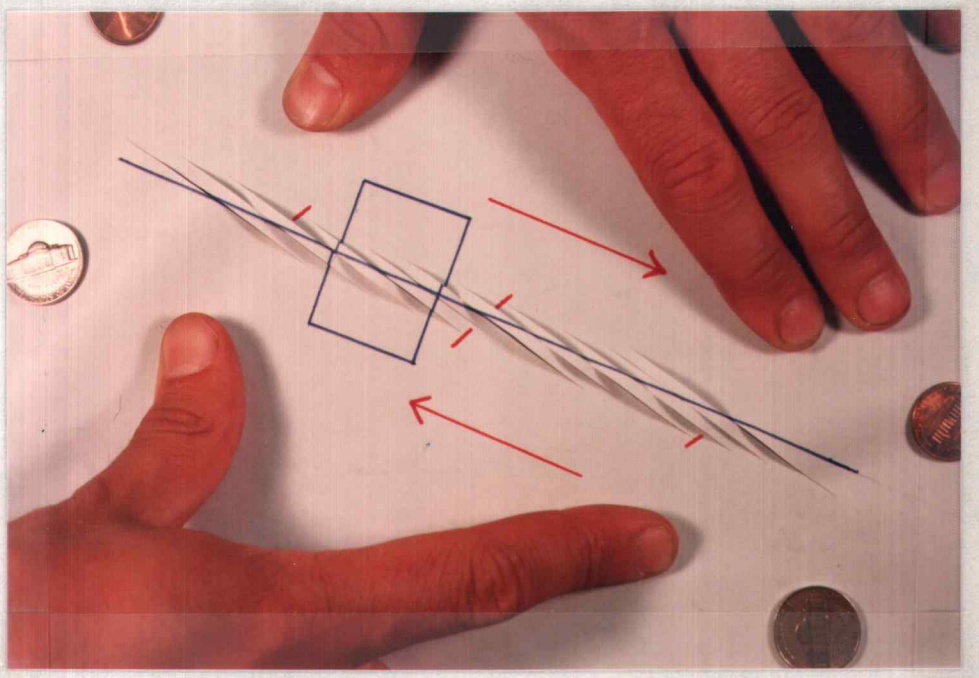

Figure 29. A simple paper model showing how normal faults are produced in a shear zone if the ends of the faults are pinned.
A. pre-deformation. B. post-deformation.

the Reidel shears form a positive angle relative to the trend of the fault zone. Since the fault pattern of the thesis area is considered to be representative of the fault pattern throughout the fault zone, the right lateral strike-slip model is assumed for all portions of the zone.

However, the Brothers fault zone cannot be attributed to a simple right lateral shear as there are several variations along the fault zone both in the faulting pattern and in the trend of the line of shear. The pattern of Reidel and conjugate Reidel shears is not consistent along the zone. Conjugate Reidel shears are abundant between Glass Butte and Pine Mountain but are scarce elsewhere in the zone. The basaltic unit in this section of the zone does not occur elsewhere along the zone (Walker and others, 1967) and may have had the proper mechanical properties for the formation of conjugate Reidel shears. This does not affect the stage or type of deformation, however.

The trend of the fault zone or lateral shear is not consistent from Steens Mountain to Black Butte. It changes direction abruptly at Glass Butte and again at Pine Mountain. In addition, the fault zone shows an apparent offset in the vicinity of Glass Butte. The zone of main faults trending from Steens Mountain to Glass Butte ends just north of Glass Butte and the next portion of the fault zone begins just south of Glass Butte. This would indicate a southward shift of the deep-seated strike-slip fault forming two separate faults (Fig. 30). The trend of the fault zone swings north at Pine Mountain and would

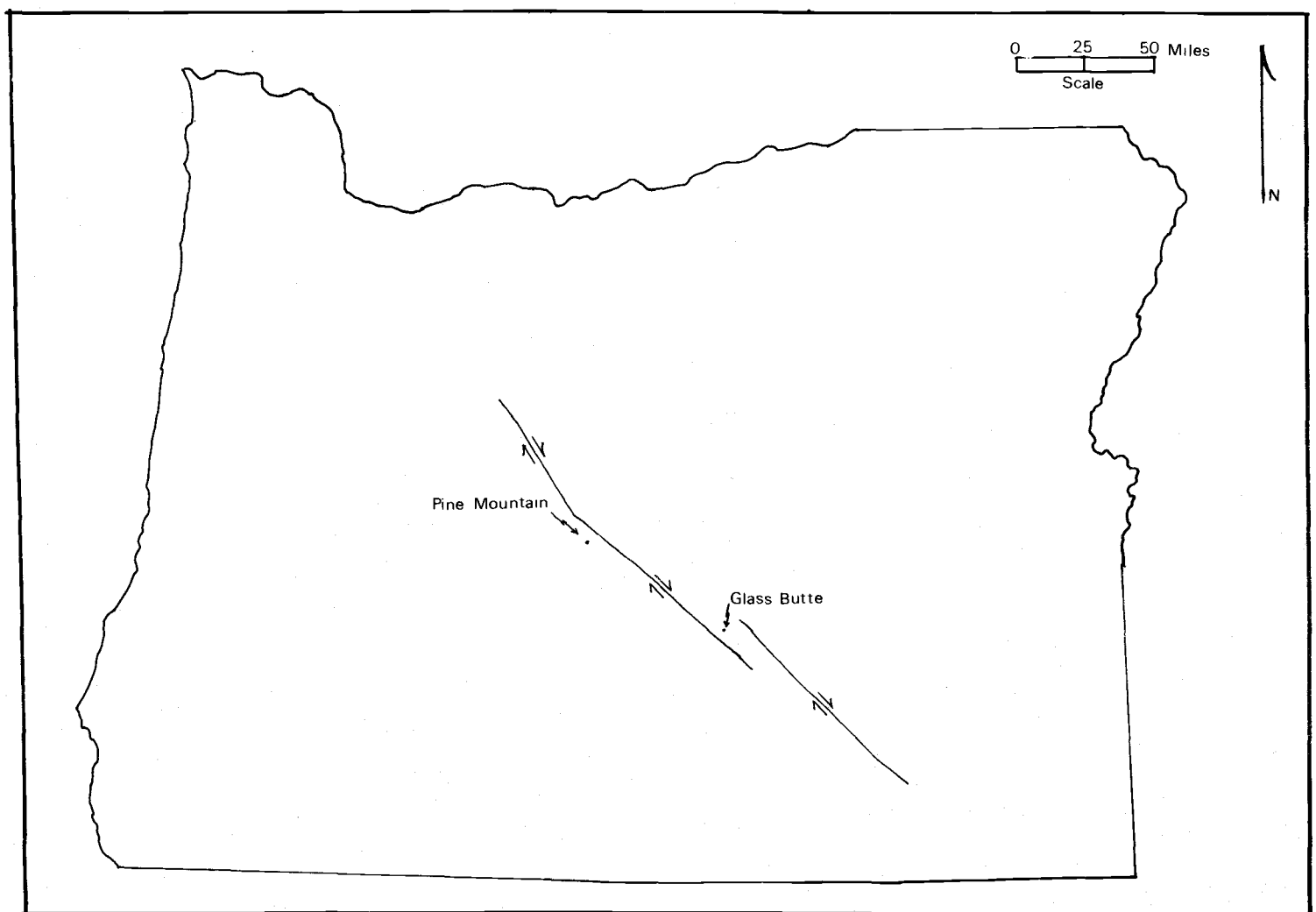

Figure 30. Postulated deep-seated structure underlying the Brothers fault zone.

indicate that the strike-slip fault changes direction there (Fig. 30).

The offset and changes in the trend of the fault zone occur in areas of large silicic domal complexes formed of flows and flow breccias, dacitic to rhyolitic in composition (Walker and others, 1967). These units show little faulting and some of the faults in the basaltic units around the domes are truncated and covered by the silicic units. It is possible these domes acted to pin the fault zone thereby deflecting its trend. However, it is more likely that the silicic volcanism is a response to the change in the deep-seated structure and tectonics as it occurred after the main stage of faulting.

Regional Relationships

The Brothers fault zone is found at the northern edge of the Basin and Range Province, an area of east-west extension shown by both normal faulting and strike-slip shear zones. The Brothers fault zone is one of several right lateral strike-slip shear zones in this area. Three others have been noted in Oregon (Lawrence, in press) and several have been described in northeastern California (Pease, 1969). The Walker Lane, another broad shear zone, extends northwest across Nevada and is considered to be slightly older than those in Oregon and California (Nielsen, 1965). The Las Vegas Valley shear zone, the Death Valley-Furnace Creek fault system, and the Stewart Valley fault are young shear zones in the southwestern part

of the Basin and Range Province (Stewart and others, 1968).

Most of these shear zones show right lateral displacement. The offset on the Soda Spring Valley fault system is estimated at ten miles (Nielsen, 1965) and the offset on the Death Valley-Furnace Creek fault system is as much as fifty miles or more (Stewart and others, 1968). The total amount of extension across the Basin and Range as indicated by both normal faulting and shear zones is estimated to be at least 60 miles (Stewart, 1971; Thompson and Burke, 1974). The Brothers fault zone shows no lateral displacement relative to the other shear zones of the Basin and Range. This may be because it forms a northern boundary of the province. The amount of extension along this boundary may be less than elsewhere in the province and further study to determine if extension decreases northward in the Basin and Range and ends along the Brothers fault zone is suggested.

There are two distinct events in the evolution of the Basin and Range Province. Calc-alkalic igneous activity began 35 to 40 million years ago and continued to the middle Tertiary. A change in the tectonic pattern, the onset of Basin and Range type faulting, occurred near the end of the Oligocene in southern New Mexico and Arizona and the change slowly migrated northwest. This change in tectonic pattern was associated with basaltic volcanism of a tholeiitic nature rather than calc-alkalic igneous activity (Christiansen and Lipman,

1972). The age of faulting along the Brothers fault zone indicates that the tectonic change reached Oregon about 15 to 16 million years ago and the northwest migration of the movement is borne out by the volcanic activity along the zone. Walker (1974) noted that the age of silicic volcanism decreased from southeast to northwest along the Brothers fault zone. A similar and mirror image trend of increasingly younger silicic volcanism from southwestern Idaho northeast along the Snake River Plain was noted by Eaton, Christiansen, and others (1975) and the correlation bears more study.

It is generally accepted that the onset of extension across the Basin and Range is associated with the convergence of the East Pacific Rise and the North American continental plate. High heat flow, anomalous upper mantle velocities, and basaltic volcanism are observed in the area of extension. Cook (1969) called for a model in which the East Pacific Rise is situated under the Basin and Range and is causing the upwelling of mantle material and the extension of the province. Thompson and Burke (1974) suggest that the thermal effects of the subduction process are still being felt in the Basin and Range because the formerly descending lithosphere is still hot. This would account for the high heat flow. In a model of Cenozoic plate tectonics in the western United States, Atwater (1970) described the Basin and Range as a wide soft boundary between two obliquely diverging rigid plates. Noble (1972) and Christiansen and Lipman (1972)

support this idea stating that the high heat flow and anomolous upper mantle seismic velocities are the effects of regional extension. Christiansen and Lipman (1972) also suggest a relationship between the Oregon plateau volcanism and extension which occurs in the foreland of the Pacific coastal orogenic and volcanic region and the extension noted by Karig (1971) that occurs behind some island arcs. This correlation may lead to a more well defined or different model for the development of the Brothers fault zone.

LIST OF REFERENCES

Atwater, Tanya, 1970, Implications of plate tectonics for the Cenozoic tectonic evolution of western North America: Geol. Soc. Am. Bull., v. 81, p. 3513-3536.

Baldwin, E. M., 1963, Geology of Oregon, 2nd. ed.: Ann Arbor, Mich., Edwards Brothers, Inc., 165 p.

Christiansen, R. L. and Lipman, P. W., 1972, Cenozoic volcanism and plate tectonic evolution of the western United States, II. Late Cenozoic: Phil. Trans. Roy. Soc. London, Ser. A 271, p. 249-284.

Cook, Kenneth, 1969, Active rift system in the Basin and Range Province: Tectanophysics, v. 8, p. 469-511.

Donath, Fred, 1962, Analysis of Basin-Range structure, south-central Oregon: Geol. Soc. Am. Bull., v. 73, p. 1-16.

Eaton, Gordon; Christiansen, Robert; and others, 1975, Magma beneath Yellowstone Park: Science, v. 188, no. 490, p. 787-796.

Goddard, E. N. and others, 1963, Rock color chart: Netherlands, Huyskes-Enschede (Distributed by Geol. Soc. Am.), n. p.

Higgins, M. W., 1969, Airfall ash and pumice lapilli deposits from Central Pumice Cone, Newberry Caldera, Oregon: U. S. Geol. Survey Prof. Paper 650-D, p. D26-D32.

Higgins, M. W. and Waters, A. C., 1967, Newberry Caldera, Oregon: a preliminary report: ORE BIN, v. 29, p. 37-60.

Karig, D. E., 1971, Origin and development of marginal basins in the western Pacific: Jour. Geophys. Res., v. 76, p. 2542-2561.

Lawrence, Robert, in press, Strike-slip faulting terminates the Basin and Range Province in Oregon.

MacDonald, G. A. and Katsura, T., 1964, Chemical composition of Hawaiian lavas: Jour. Petrol., v. 5, p. 82-133.

Nielsen, R. L., 1965, Right-lateral strike-slip faulting in the Walker Lane, west-central Nevada: Geol. Soc. Am. Bull., v. 76, p. 1301-1308.

Noble, Donald, 1972, Some observations on the Cenozoic volcano-tectonic evolution of the Great Basin, western United States: Earth and Planetary Sci. Letters, v. 17, p. 142-150.

Pease, Robert, 1969, Normal faulting and lateral shear in north-eastern California: Geol. Soc. Am. Bull., v. 80, p. 715-720.

Stewart, J. H., 1971, Basin and Range structure: a system of horsts and grabens produced by deep-seated extension: Geol. Soc. Am. Bull., v. 82, p. 1019-1044.

Stewart, J. H., Albers, J. P., and Poole, F. G., 1968, Summary of regional evidence for right-lateral displacement in the Western Great Basin: Geol. Soc. Am. Bull., v. 79, p. 1407-1414.

Stewart, J. H., Walker, G. W., and Kleinhampl, F. J., 1975, Oregon-Nevada lineament: Geology, v. 3, no. 5, p. 165-168.

Taylor, E. M., 1975, Professor of Geology, Oregon State University, personal communication.

Tchalenko, J. S., 1970, Similarities between shear zones of different magnitudes: Geol. Soc. Am. Bull., v. 81, p. 1625-1640.

Tchalenko, J. S. and Ambraseys, N. N., 1970, Structural analysis of the Dasht-e Bayaz (Iran) earthquake fractures: Geol. Soc. Am. Bull., v. 81, p. 41-60.

Thompson, George and Burke, Dennis, 1974, Regional geophysics of the Basin and Range Province: p. 213-238 in Donath, ed.: Annual Review of Earth and Planetary Sci., 478 p.

Walker, G. W., 1969, Geology of the High Lava Plains Province, in Mineral and water resources of Oregon: State Dept. Geol. and Min. Ind., Bull. 64, 1. 77-79.

_____, 1974, Some implications of late Cenozoic volcanism to geothermal potential in the High Lava Plains of south-central Oregon: ORE BIN, v. 36, no. 7, p. 1-11.

Walker, G. W., Dalrymple, G. B., and Lanphere, M. A., 1974, Index to potassium-argon ages of Cenozoic volcanic rocks of Oregon: U. S. Geol. Survey Misc. Field Studies MF- 569, Scale 1:100, 000.

Walker, G. W., Peterson, N. V., and Greene, R. C., 1967, Reconnaissance geologic map of the east half of the Crescent quadrangle; Lake, Deschutes, and Crook Counties, Oregon: U. S. Geol. Survey Misc. Geol. Inv., Map I-493, scale 1:250, 000.

Waters, A. C., 1962, Basalt magma types and their tectonic associations: Pacific northwest of the United States, in The crust of the Pacific Basin: Am. Geophys. Union Geophys., Mon. 6, p. 158-170.

Williams, Howell; Turner, Francis; and Gilbert, Charles, 1954, Petrography: an introduction to the study of rocks in thin section: San Francisco, Calif., W. H. Freeman and Company, 406 p.

APPENDICES

APPENDIX I

Chemical Analyses

TABLE A1-1

Older Basaltic Unit

Sample #	89	132	30	145	101
SiO_2	52. 1	53. 4	54. 2	55. 1	57. 6
Al_2O_3	16. 1	16. 3	15. 8	16. 2	16. 1
FeO	11. 2	10. 8	10. 2	9. 5	8. 3
MgO	4. 9	4. 2	4. 9	4. 7	4. 5
TiO_2	1. 50	1. 55	1. 30	1. 25	1. 00
CaO	8. 6	8, 4	7. 0	7. 3	6. 9
Na_2O	3. 8	4. 2	3. 5	3. 8	3. 6
K_2O	0. 90	0. 95	1. 65	1. 55	1. 30

#89 Porphyritic olivine basaltic andesite.

#132 Porphyritic basaltic andesite.

#30 Fine grained basaltic andesite.

#145 Fine grained basaltic andesite.

#101 Fine grained basaltic andesite.

Table A1-1 (cont'd)

	Younger Basaltic Unit		Dacites	
Sample #	72	39	2	100
SiO_2	51.0	54.5	70.2	73.0
Al_2O_3	15.7	16.1	15.0	15.0
FeO	9.5	10.1	3.4	2.5
MgO	9.0	4.9	0.2	0.5
TiO_2	1.15	1.25	0.10	0.25
CaO	9.5	7.2	1.4	2.3
Na_2O	3.1	3.8	5.4	3.6
K_2O	0.40	1.45	2.95	2.50

#72 Olivine-bearing diktytaxitic basalt.

#39 Olivine-bearing basaltic andesite.

#2 "Olivine-bearing" rhyodacite. (Older dacite).

#100 Hypersthene-bearing rhyodacite. (Younger dacite).

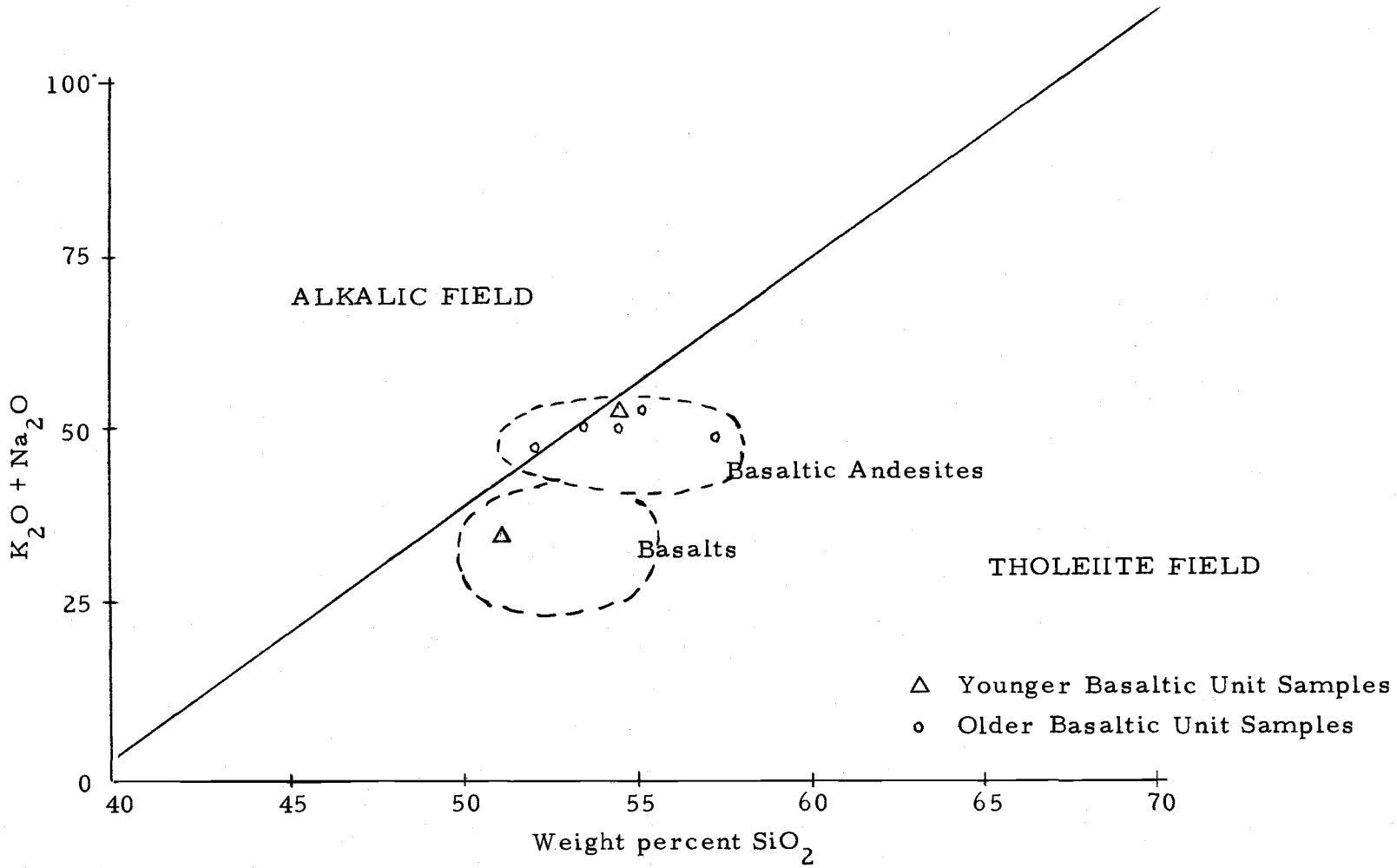

Figure A1-1. MacDonald and Katsura graph for the separation of alkalic and tholeiitic lavas.

APPENDIX II

Mechanical Behavior of Selected Rocks

A study of the mechanical behavior of selected rock samples from the thesis area reveals varied responses of the different types to stress. Experiments were performed on samples TC, TF, and QT by E. Tucker and R. Lawrence and on sample 461 by R. Lawrence. All experiments were carried out on the OSU Donath triaxial deformation apparatus. Each sample was deformed under varying confining pressures. Stress-strain curves, the Mohr-Coulomb equation of failure, and Young's modulus were calculated for each.

The behavior of the rocks in response to stress varies from very brittle faulting to ductile faulting. Sample TC, from the coarse-grained member of the older basaltic unit, is very brittle (Fig. A2-1) and a high stress (5. 5 to 6. 5 kbars) was required to cause faulting. Sample TF, from the fine-grained member of the older basaltic unit, is less brittle and under high confining pressures deforms ductilely (Fig. A2-2). The younger basaltic unit, represented by QT shows very interesting behavior (Fig. A2-3). After an initial fault is formed, there is a period of strain hardening followed by another fault. This pattern is repeated more than once in each test. The faults formed are probably conjugate faults because the cores show no throughgoing fractures (Fig. A2-5). This phenomenon is

probably the result of the vesicular nature of the samples. Sample 461, from the coarse-grained member of the older basaltic unit, was added here because it is vesicular and shows much the same behavior as the diktytaxitic younger basaltic unit (Fig. A2-4). Both these samples also exhibit much strain hardening. A further study of these vesicular rocks would be interesting to see what effect pores and pore pressure changes have on their mechanical behavior,

The Mohr-Coulomb equation of failure was calculated for each group of samples (construction not shown) and the equations are written on each graph. In the construction, several Mohr circles did not fit the line and were discarded on the basis that vesicles or phenocrysts in each caused irregularities.

Young's modulus was calculated for each experiment performed to show the linear relationship between the stress and elastic strain. This value, E, varies for each experiment and within each sample and is probably dependent upon the minor irregularities in each sample as well as on the change in mechanical behavior relative to the confining pressure (P_c). See Table A2-1.

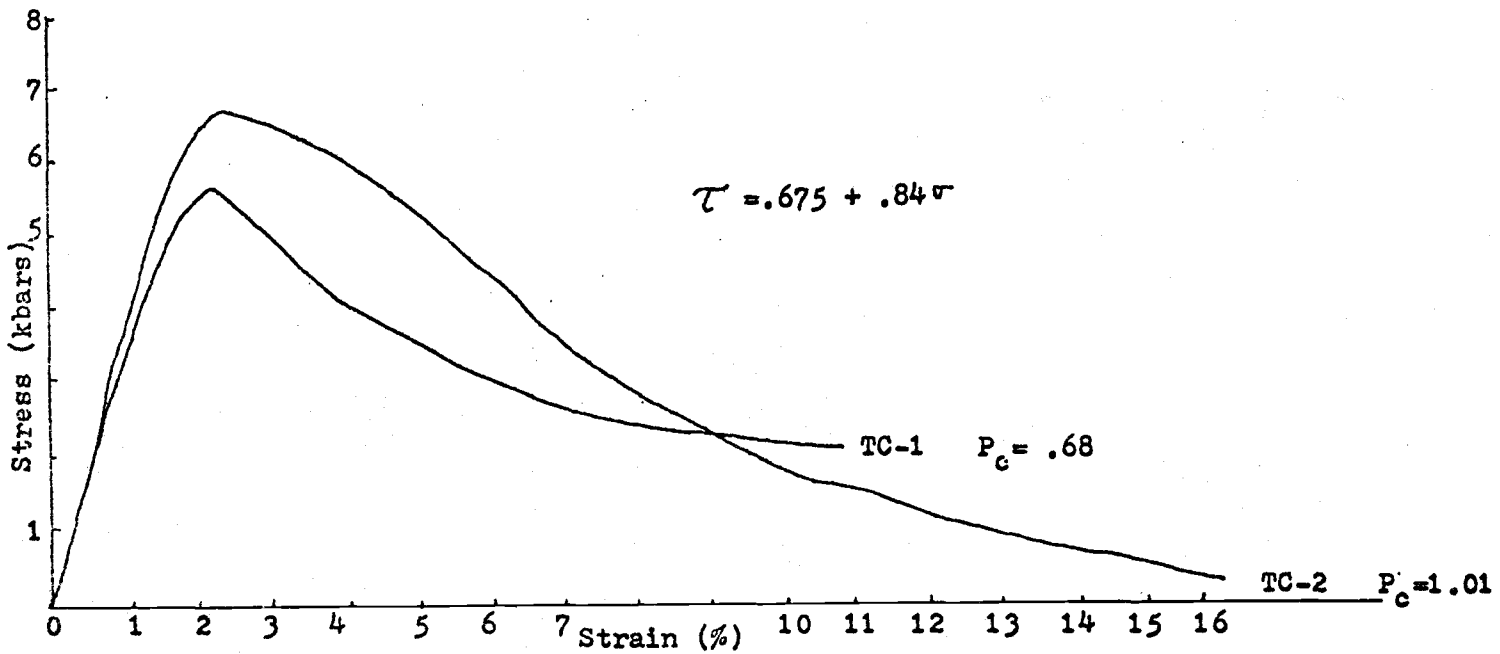

Figure A2-1. Stress-strain curve for sample TC.
Coarse-grained olivine-bearing basaltic rock.

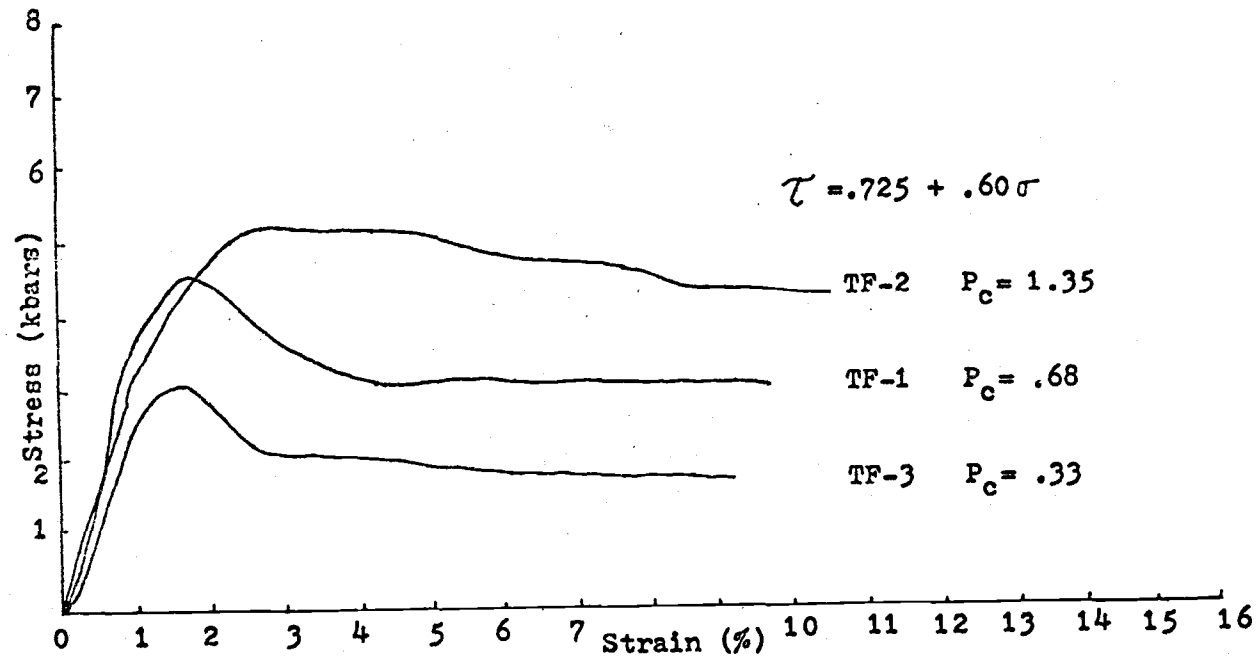

Figure A2-2. Stress-strain curve for sample TF. Fine-grained basaltic andesite.

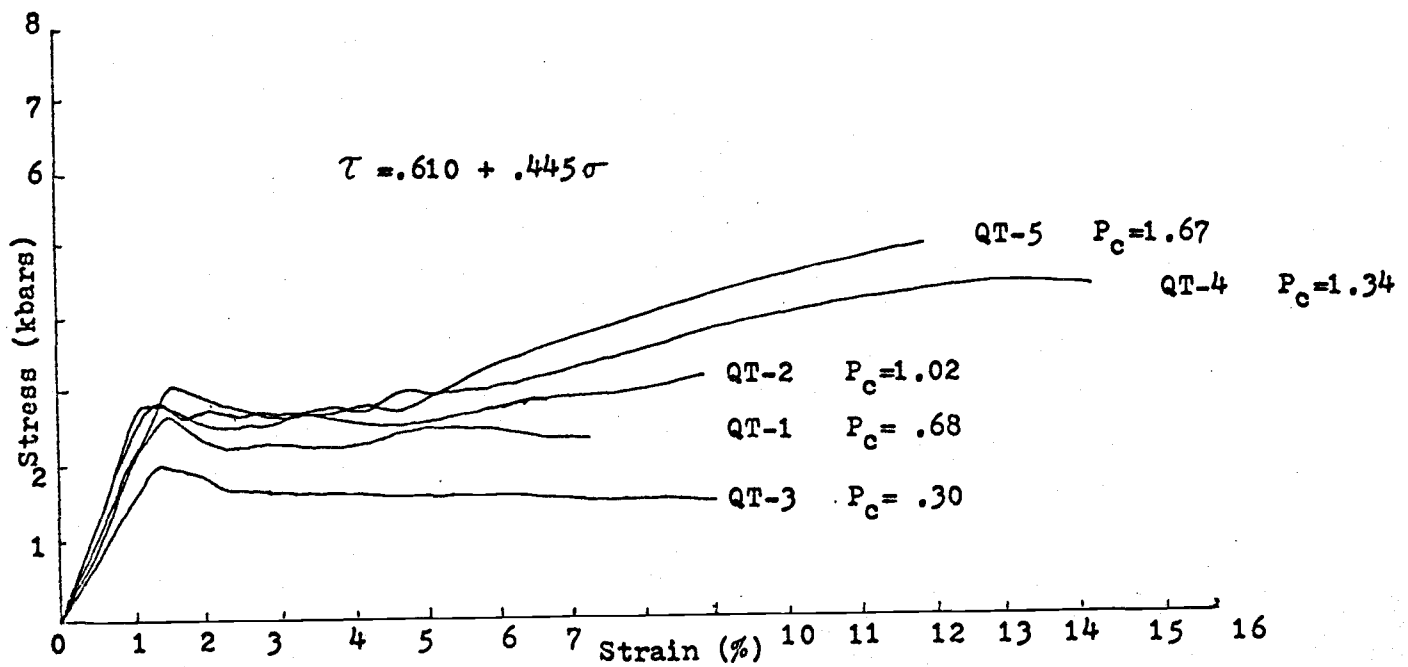

Figure A2-3. Stress-strain curve for sample QT.
Diktytaxitic olivine-bearing basaltic rock.

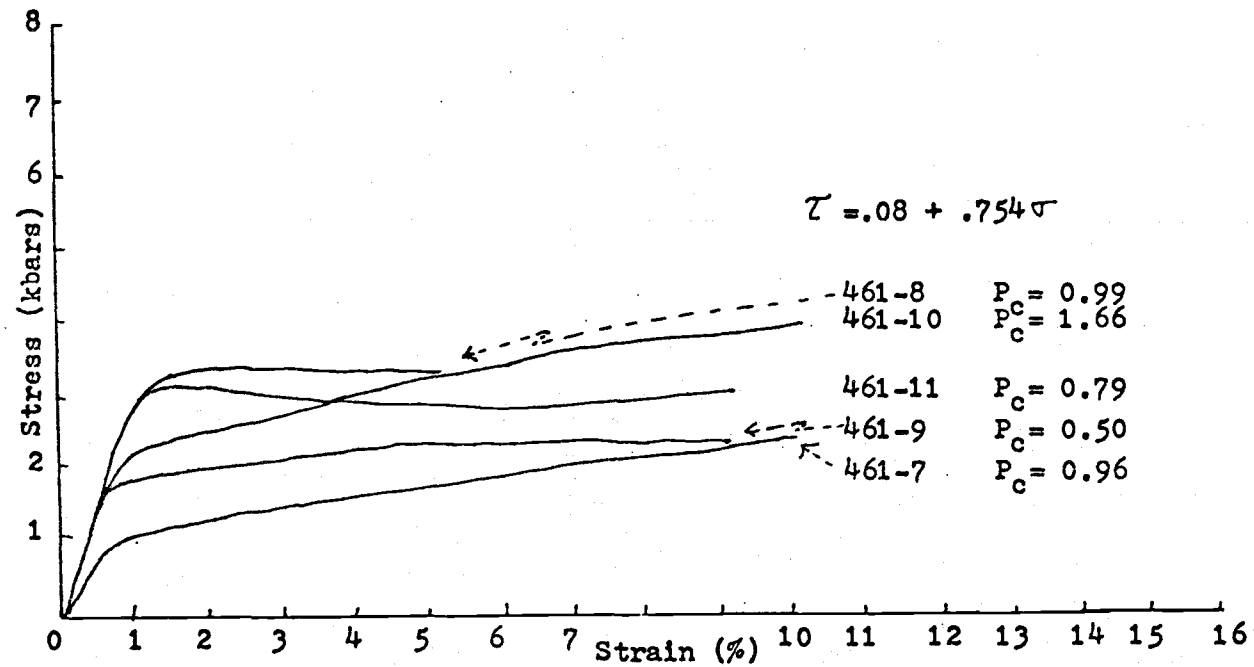

Figure A2-4. Stress-strain curve for sample 461.
Vesicular coarse-grained olivine basaltic rock.

A.

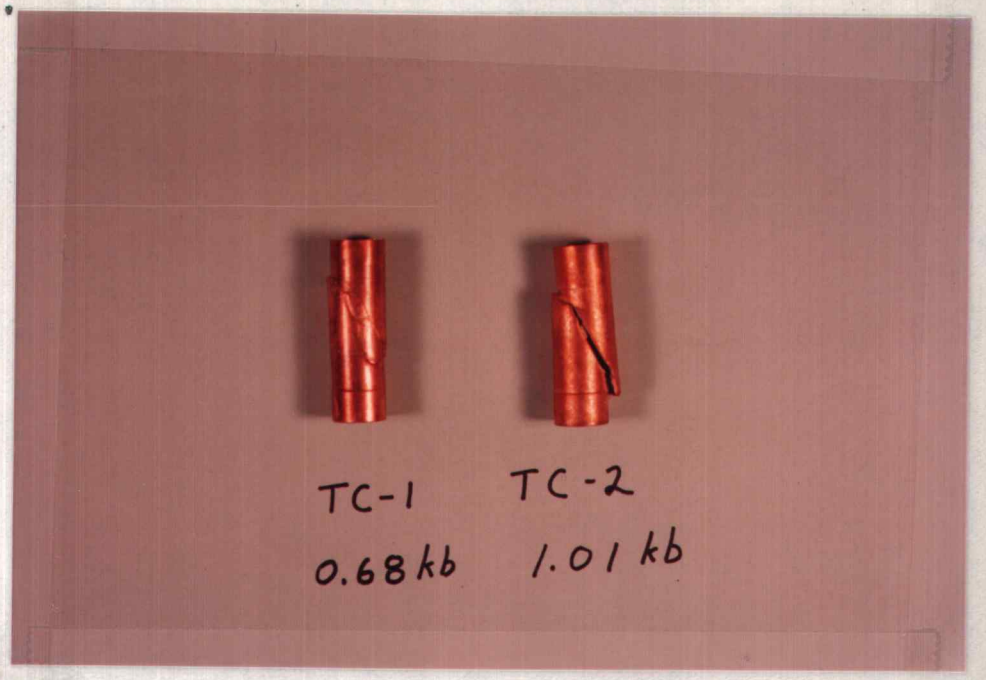

B.

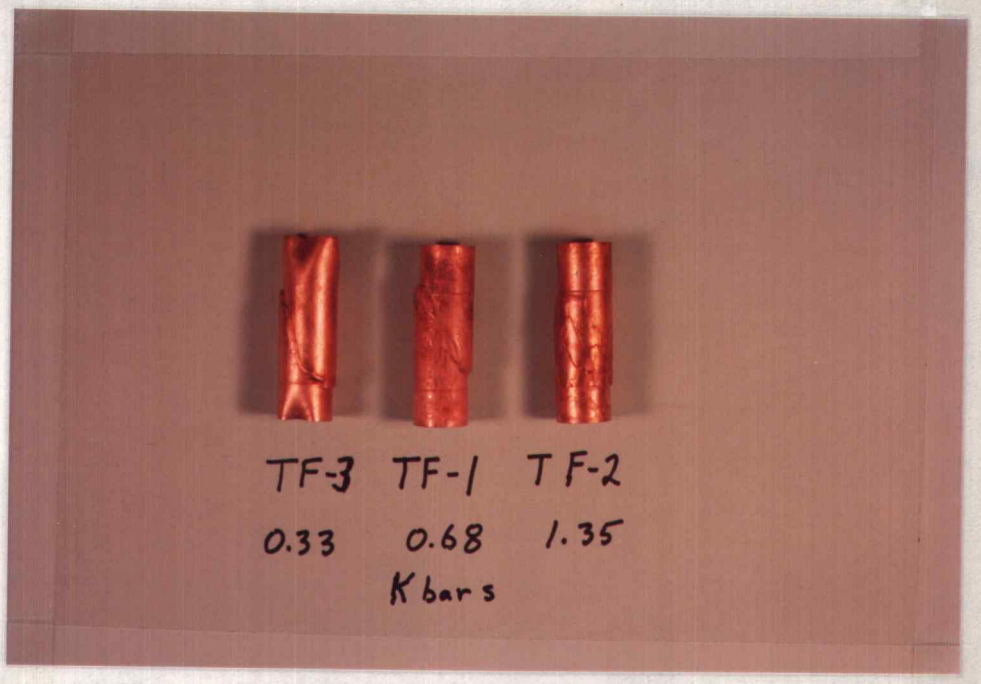

Figure A2-5. A. Cores of sample TC.
B. Cores of sample TF.

C.

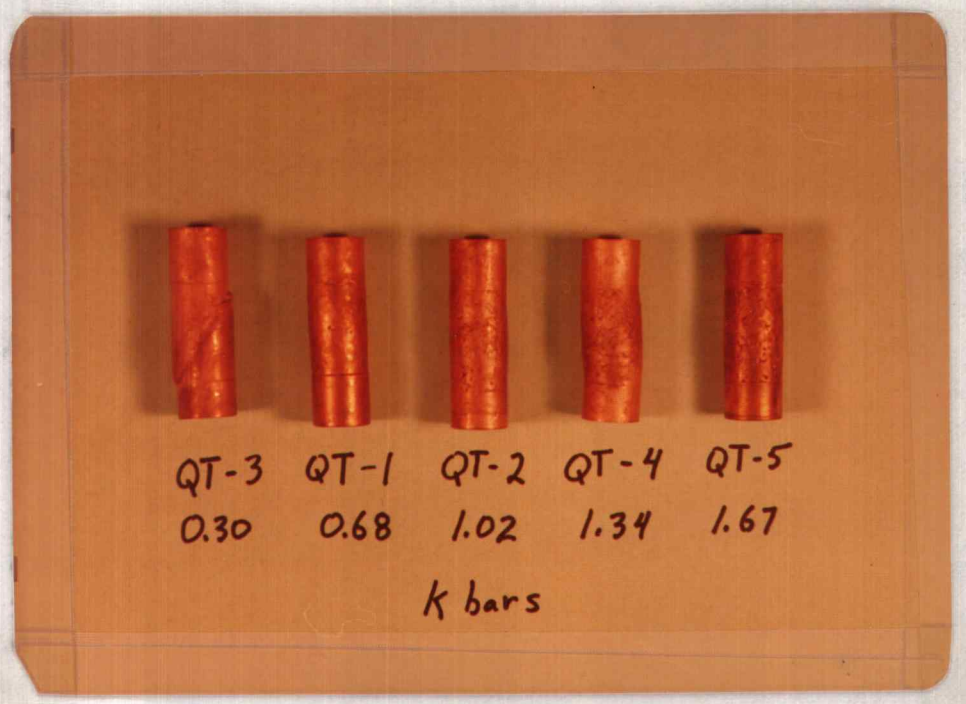

Figure A2-5. C. Cores of sample QT.

Table A2-1
Young's Modulus (E)

Sample	P_c Values	E Values
TC-1	.68	3.13
TC-2	1.01	3.11
TF-3	.33	2.30
TF-1	.68	3.61
TF-2	1.35	2.62
QT-3	.30	1.84
QT-1	.68	2.20
QT-2	1.02	2.20
QT-4	1.34	2.13
QT-5	1.67	2.66

APPARATUS 733
SAMPLE NO. TC 1
DATE 06/16/75
OPERATOR TUCKER

CONSTANTS

K1(IN./LB.) = 1.700E-06
K2 (LB./DIV.) = 200.0
K3 (IN./LB.) = 1.000E-03
K4 (IN./LB.) = 7.500E-07

RECORDED BEFORE RUN		RECORDED AFTER RUN	
TEMPERATURE (DEGREES C.)	25.0	D(SAT)	-12.0
PORE PRESSURE (PSI)	15.0	D(SCP)	0
CONFINING PRESSURE (K-BARS)	.68	D(RSCP)	54.0
ANISOTROPY	0	D(RSAT)	39.0
SAMPLE LENGTH (IN.)	1.0800	L(FR0)	-49.0
SAMPLE DIAMETER (IN.)	.4920	L(F0)	0

CALCULATED

V(0) (CU.IN.)	.2053	E(CP) (PERCENT)	.43
L(CP) (IN.)	1.0753	E(PAT) (PERCENT)	4.63
L(F) (IN.)	1.0519	E(PCP) (PERCENT)	5.02
V(CP) (CU.IN.)	.2027	E(ECP) (PERCENT)	5.72
A(F) (SQ.IN.)	.1927	P(C) (K-BARS)	.68

NO.	D(I)	L(I)	STRESS (K-BARS)	STRAIN (%)	
1:	0	0	0	0	
2:	5.0	9.0	.657	.180	EA
3:	15.0	26.0	1.890	.573	
4:	25.0	43.0	3.114	.965	EB
5:	35.0	60.0	4.328	1.359	
6:	40.0	68.0	4.895	1.570	
7:	45.0	74.0	5.312	1.845	
8:	50.0	78.0	5.580	2.183	EF
9:	55.0	68.0	4.864	2.965	
10:	60.0	58.0	4.149	3.746	
11:	71.0	50.0	3.577	4.929	
12:	80.0	42.0	3.004	6.111	
13:	90.0	37.0	2.647	7.200	
14:	100.0	34.0	2.432	8.224	
15:	110.0	33.0	2.361	9.186	
16:	120.0	32.0	2.289	10.147	
17:	126.0	31.0	2.217	10.737	EZ

APPARATUS 733
SAMPLE NO. TC 2
DATE 06/16/75
OPERATOR TUCKER

CONSTANTS

K1(IN./LB.) = 1.700E-06
K2 (LB./DIV.) = 200.0
K3 (IN./LB.) = 1.000E-03
K4 (IN./LB.) = 7.500E-07

RECORDED BEFORE RUN		RECORDED AFTER RUN	
TEMPERATURE (DEGREES C.)	25.0	D(SAT)	-14.0
PORE PRESSURE (PSI)	15.0	D(SCP)	0
CONFINING PRESSURE (K-BARS)	1.01	D(RSCP)	200.0
ANISOTROPY	C	D(RSAT)	176.0
SAMPLE LENGTH (IN.)	1.0700	L(FR0)	-73.0
SAMPLE DIAMETER (IN.)	.4920	L(F)	0

CALCULATED

V(0) (CU.IN.)	.2034	E(CP) (PERCENT)	.29
L(CP) (IN.)	1.0670	E(PAT) (PERCENT)	17.76
L(F) (IN.)	.9873	E(PCP) (PERCENT)	18.75
V(CP) (CU.IN.)	.2017	E(FCP) (PERCENT)	-0.56
A(F) (SQ.IN.)	.2043	P(C) (K-BARS)	1.01

NO.	D(I)	L(I)	STRESS (K-BARS)	STRAIN (%)	
1:	0	0	0	0	
2:	5.0	9.0	.655	.182	
3:	15.0	27.0	1.959	.545	=A
4:	25.0	45.0	3.251	.909	
5:	35.0	64.0	4.609	1.241	
6:	45.0	80.0	5.736	1.668	
7:	50.0	87.0	6.222	1.914	=B
8:	55.0	93.0	6.633	2.191	
9:	60.0	92.0	6.528	2.692	
10:	65.0	89.0	6.278	3.256	
11:	75.0	80.0	5.572	4.480	
12:	95.0	45.0	3.036	7.470	=F
13:	115.0	28.0	1.889	9.886	
14:	135.0	18.0	1.214	12.079	
15:	145.0	15.0	1.012	13.112	
16:	150.0	12.0	.810	13.676	
17:	155.0	10.0	.675	14.209	
18:	160.0	8.0	.540	14.741	
19:	165.0	7.0	.472	15.242	
20:	175.0	5.0	.337	16.243	
21:	185.0	4.0	.270	17.212	
22:	195.0	3.0	.202	18.181	=Z

APPARATUS 733
SAMPLE NO. TF-1
DATE 06/13/75
OPERATOR TUCKER

CONSTANTS

K1(IN./LB.) = 1.700E-06
K2 (LB./DIV.) = 200.0
K3 (IN./LB.) = .0010
K4 (IN./LB.) = 7.500E-07

RECORDED BEFORE RUN		RECORDED AFTER RUN	
TEMPERATURE (DEGREES C.)	25.0	D(SAT)	-8.0
PORE PRESSURE (PSI)	15.0	D(SCP)	0
CONFINING PRESSURE (K-BARS)	.68	D(RSCP)	79.0
ANISOTROPY	0	D(RSAT)	65.0
SAMPLE LENGTH (IN.)	.9950	L(FR0)	-49.0
SAMPLE DIAMETER (IN.)	.4920	L(FR)	0

CALCULATED

V(0) (CU.IN.)	.1892	E(CP) (PERCENT)	.07
L(CP) (IN.)	.9943	E(PAT) (PERCENT)	7.34
L(F) (IN.)	.9727	E(PCP) (PERCENT)	7.94
V(CP) (CU.IN.)	.1888	E(ECP) (PERCENT)	1.63
A(F) (SQ.IN.)	.1941	P(C) (K-BARS)	.68

NO.	D(I)	L(I)	STRESS (K-BARS)	STRAIN (%)	
1:	0	0	0	0	
2:	3.0	3.0	.217	.199	
3:	4.0	7.0	.507	.163	-A
4:	6.0	11.0	.797	.227	
5:	9.0	16.0	1.157	.358	
6:	12.0	21.0	1.517	.489	
7:	14.0	26.0	1.878	.519	
8:	17.0	31.0	2.236	.650	
9:	19.0	35.0	2.523	.714	
10:	21.0	40.0	2.882	.744	
11:	24.0	44.0	3.165	.909	-B
12:	26.0	47.0	3.378	1.008	
13:	29.0	51.0	3.659	1.173	
14:	32.0	56.0	4.012	1.303	
15:	34.0	58.0	4.150	1.436	
16:	36.0	59.0	4.214	1.603	
17:	37.0	61.0	4.356	1.635	
18:	39.0	61.0	4.347	1.836	
19:	41.0	61.0	4.338	2.038	

20:	42.0	60.0	4.261	2.172	<-F
21:	43.0	59.0	4.198	2.387	
22:	44.0	56.0	3.977	2.510	
23:	46.0	53.0	3.764	2.814	
24:	47.0	51.0	3.622	2.983	
25:	49.0	58.0	4.119	2.945	
26:	50.0	46.0	3.267	3.456	
27:	52.0	45.0	3.196	3.691	
28:	54.0	44.0	3.125	3.926	
29:	57.0	43.0	3.054	4.262	
30:	59.0	42.0	2.983	4.497	
31:	61.0	42.0	2.983	4.699	
32:	64.0	42.0	2.983	5.000	
33:	67.0	42.5	3.018	5.285	
34:	69.0	42.5	3.018	5.486	
35:	74.0	41.0	2.912	6.040	
36:	79.0	41.0	2.912	6.543	
37:	84.0	41.0	2.912	7.046	
38:	89.0	41.0	2.912	7.549	
39:	94.0	41.0	2.912	8.051	
40:	99.0	40.5	2.876	8.571	
41:	104.0	40.5	2.876	9.074	
42:	109.0	40.5	2.876	9.577	<-Z

APPARATUS 733
SAMPLE NO. TF-2
DATE 06/13/75
OPERATOR TUCKER

CONSTANTS

K1(IN./LB.) = 1.700E-06
K2 (LB./DIV.) = 200.0
K3 (IN./LB.) = .0010
K4 (IN./LB.) = 7.500E-07

RECORDED BEFORE RUN		RECORDED AFTER RUN	
TEMPERATURE (DEGREES C.)	25.0	D(SAT)	-16.0
PORE PRESSURE (PSI)	15.0	D(SCP)	0
CONFINING PRESSURE (K-BARS)	1.35	D(RSCP)	78.0
ANISOTROPY	0	D(RSAT)	61.0
SAMPLE LENGTH (IN.)	.9755	L(FR0)	-98.0
SAMPLE DIAMETER (IN.)	.4920	L(FR)	0

CALCULATED

V(B) (CU.IN.)	.1855	E(CP) (PERCENT)	.13
L(CP) (IN.)	.9742	E(PAT) (PERCENT)	7.89
L(F) (IN.)	.9437	E(PCP) (PERCENT)	8.01
V(CP) (CU.IN.)	.1847	E(ECP) (PERCENT)	2.29
A(F) (SQ.IN.)	.1957	P(C) (K-BARS)	1.35

NO.	D(I)	L(I)	STRESS (K-BARS)	STRAIN (%)	
1:	0	0	0	0	
2:	3.0	5.0	.363	.133	
3:	5.0	9.0	.653	.199	-A
4:	7.0	13.0	.943	.265	
5:	10.0	17.0	1.230	.433	
6:	12.0	21.0	1.519	.499	
7:	14.0	25.0	1.807	.565	
8:	16.0	28.0	2.022	.665	
9:	18.0	32.0	2.309	.731	
10:	21.0	37.0	2.666	.864	
11:	23.0	40.0	2.880	.965	
12:	25.0	42.0	3.020	1.100	-B
13:	26.0	45.0	3.235	1.098	
14:	28.0	47.0	3.374	1.234	
15:	31.0	52.0	3.728	1.367	
16:	34.0	56.0	4.008	1.536	
17:	36.0	59.0	4.219	1.636	
18:	38.0	61.0	4.356	1.772	
19:	39.0	62.0	4.424	1.839	
20:	41.0	64.0	4.561	1.975	
21:	42.0	65.0	4.629	2.043	
22:	44.0	67.0	4.764	2.178	
23:	46.0	69.0	4.900	2.314	
24:	48.0	70.5	4.999	2.467	
25:	49.0	71.0	5.030	2.552	
26:	51.0	71.5	5.055	2.740	
27:	53.0	72.0	5.081	2.928	
28:	55.0	72.0	5.070	3.133	-F
29:	57.0	71.5	5.035	3.356	
30:	59.0	71.5	5.035	3.561	
31:	61.0	71.0	5.000	3.784	
32:	64.0	71.0	5.000	4.092	
33:	67.0	71.0	5.000	4.400	
34:	69.0	71.0	5.000	4.605	
35:	71.0	70.5	4.964	4.828	
36:	73.0	70.0	4.929	5.050	
37:	75.0	69.5	4.894	5.273	
38:	77.0	69.0	4.859	5.496	
39:	80.0	68.5	4.824	5.821	
40:	83.0	68.0	4.788	6.147	
41:	86.0	67.5	4.753	6.472	
42:	89.0	67.0	4.718	6.797	

43:	92.0	67.0	4.718	7.105
44:	94.0	66.5	4.683	7.328
45:	98.0	66.0	4.648	7.756
46:	100.0	66.0	4.648	7.961
47:	103.0	55.5	3.908	8.636
48:	106.0	55.5	3.908	8.944
49:	109.0	55.5	3.908	9.252
50:	111.0	55.5	3.908	9.457
51:	115.0	55.0	3.873	9.885
52:	119.0	55.0	3.873	10.296 -Z

APPARATUS 733
SAMPLE NO. TF-3
DATE 06/13/75
OPERATOR TUCKER

CONSTANTS

K1(IN./LB.) = 1.700E-06
K2 (LB./DIV.) = 200.0
K3 (IN./LB.) = .0010
K4 (IN./LB.) = 7.500E-07

RECORDED BEFORE RUN		RECORDED AFTER RUN	
TEMPERATURE (DEGREES C.)	25.0	D(SAT)	-4.0
PORE PRESSURE (PSI)	15.0	D(SCP)	0
CONFINING PRESSURE (K-BARS)	.33	D(RSCP)	89.0
ANISOTROPY	0	D(RSAT)	78.0
SAMPLE LENGTH (IN.)	.9900	L(FR0)	-24.0
SAMPLE DIAMETER (IN.)	.4920	L(FR)	0

CALCULATED

V(0) (CU.IN.)	.1882	E(CP) (PERCENT)	.04
L(CP) (IN.)	.9896	E(PAT) (PERCENT)	8.28
L(F) (IN.)	.9725	E(PCP) (PERCENT)	8.99
V(CP) (CU.IN.)	.1880	E(ECP) (PERCENT)	.42
A(F) (SQ.IN.)	.1933	P(C) (K-BARS)	.33

NO.	D(I)	L(I)	STRESS (K-BARS)	STRAIN (%)
1:	0	0	0	0
2:	3.0	3.0	.217	.200
3:	5.0	6.0	.434	.299 -A
4:	10.0	15.0	1.083	.495

5:	15.0	23.0	1.657	.726	
6:	20.0	31.0	2.228	.956	
7:	25.0	38.0	2.724	1.221	-B
8:	28.0	40.0	2.868	1.455	
9:	29.0	41.0	2.930	1.522	
10:	31.0	41.0	2.924	1.724	-F
11:	38.0	28.0	1.997	2.878	
12:	40.0	28.0	1.997	3.080	
13:	43.0	28.0	1.997	3.383	
14:	45.0	28.0	1.997	3.585	
15:	49.0	28.0	1.997	3.989	
16:	51.0	27.0	1.925	4.226	
17:	55.0	27.0	1.925	4.630	
18:	60.0	26.0	1.854	5.170	
19:	65.0	25.5	1.818	5.692	
20:	70.0	25.0	1.783	6.215	
21:	75.0	24.5	1.747	6.737	
22:	80.0	24.0	1.711	7.259	
23:	84.0	24.0	1.711	7.664	
24:	90.0	24.0	1.711	8.270	
25:	95.0	24.0	1.711	8.775	
26:	100.0	23.5	1.676	9.298	
27:	101.0	23.0	1.640	9.416	-Z

APPARATUS 733
SAMPLE NO. QT 1
DATE 06/16/75
OPERATOR TUCKER

CONSTANTS

K1(IN./LB.) = 1.700E-06
K2 (LB./DIV.) = 200.0
K3 (IN./LB.) = 1.000E-03
K4 (IN./LB.) = 7.500E-07

RECORDED BEFORE RUN		RECORDED AFTER RUN	
TEMPERATURE (DEGREES C.)	25.0	D(SAT)	-9.0
PORE PRESSURE (PSI)	0	D(SCP)	0
CONFINING PRESSURE (K-BARS)	.68	D(RSCP)	58.0
ANISOTROPY	0	D(RSAT)	44.0
SAMPLE LENGTH (IN.)	.9610	L(FR0)	-49.0
SAMPLE DIAMETER (IN.)	.4920	L(FR)	0

CALCULATED

V(0) (CU.IN.)	.1827	E(CP) (PERCENT)	.17
L(CP) (IN.)	.9593	E(PAT) (PERCENT)	5.52
L(F) (IN.)	.9449	E(PCP) (PERCENT)	6.05
V(CP) (CU.IN.)	.1813	E(CCP) (PERCENT)	1.21
A(F) (SQ.IN.)	.1934	P(C) (K-BARS)	.68

NO.	D(I)	L(I)	STRESS (K-BARS)	STRAIN (%)	
1:	0	0	0	0	
2:	5.0	8.0	.581	.239	EA
3:	7.0	11.0	.798	.340	
4:	10.0	15.0	1.158	.475	
5:	14.0	21.0	1.517	.715	
6:	17.0	26.0	1.875	.851	
7:	20.0	31.0	2.233	.986	EB
8:	22.0	33.0	2.374	1.124	
9:	24.0	35.0	2.514	1.261	
10:	25.0	37.0	2.657	1.295	
11:	26.0	38.0	2.727	1.363	
12:	27.0	37.0	2.651	1.503	EF
13:	29.0	36.0	2.580	1.643	
14:	29.0	35.0	2.508	1.792	
15:	30.0	33.0	2.365	1.958	
16:	31.0	32.0	2.293	2.097	
17:	32.0	32.0	2.293	2.201	
18:	34.0	32.0	2.293	2.410	
19:	36.0	32.0	2.293	2.618	
20:	39.0	32.5	2.329	2.809	
21:	40.0	33.0	2.365	3.000	
22:	42.0	33.0	2.365	3.218	
23:	44.0	32.0	2.293	3.452	
24:	46.0	31.5	2.257	3.679	
25:	48.0	32.0	2.293	3.869	
26:	50.0	33.0	2.365	4.042	
27:	52.0	33.5	2.400	4.233	
28:	54.0	34.0	2.436	4.424	
29:	56.0	35.0	2.508	4.597	
30:	58.0	35.0	2.508	4.805	
31:	60.0	35.5	2.544	4.996	
32:	62.0	35.5	2.544	5.205	
33:	64.0	35.5	2.544	5.413	

34:	66.0	35.0	2.580	5.604	
35:	68.0	36.0	2.580	5.812	
36:	70.0	35.0	2.508	6.056	
37:	72.0	34.0	2.436	6.300	
38:	74.0	33.5	2.400	6.526	
39:	76.0	33.0	2.365	6.752	
40:	78.0	33.0	2.365	6.961	
41:	80.0	33.5	2.400	7.152	
42:	81.0	33.5	2.400	7.256	=Z

APPARATUS 733
SAMPLE NO. QT 2
DATE 06/16/75
OPERATOR TUCKER

CONSTANTS

K1(IN./LB.) = 1.700E-06
K2 (LB./DIV.) = 200.0
K3 (IN./LB.) = 1.000E-03
K4 (IN./LB.) = 7.500E-07

RECORDED BEFORE RUN		RECORDED AFTER RUN	
TEMPERATURE (DEGREES C.)	25.0	D(SAT)	-11.0
PORE PRESSURE (PSI)	0	D(SCP)	0
CONFINING PRESSURE (K-BARS)	1.02	D(RSCP)	71.0
ANISOTROPY	0	D(RSAT)	50.0
SAMPLE LENGTH (IN.)	.9620	L(FR0)	-74.0
SAMPLE DIAMETER (IN.)	.4920	L(FR)	0

CALCULATED

V(0) (CU.IN.)	.1829	E(CP) (PERCENT)	-0.01
L(CP) (IN.)	.9621	E(SAT) (PERCENT)	6.34
L(F) (IN.)	.9479	E(PCP) (PERCENT)	7.38
V(CP) (CU.IN.)	.1929	E(CCP) (PERCENT)	1.32
A(F) (SQ.IN.)	.1930	P(C) (K-BARS)	1.02

NO.	D(I)	L(I)	STRESS (K-BARS)	STRAIN (%)	
1:	0	0	0	0	
2:	5.0	8.0	.579	.237	=A
3:	7.0	11.0	.796	.339	
4:	10.0	15.0	1.082	.509	
5:	13.0	20.0	1.440	.644	
6:	16.0	26.0	1.871	.744	
7:	20.0	31.0	2.225	.983	=B
8:	23.0	36.0	2.580	1.118	
9:	25.0	39.0	2.792	1.220	
10:	27.0	42.0	3.004	1.322	
11:	28.0	43.0	3.074	1.391	
12:	29.0	43.5	3.107	1.477	=F
13:	30.0	43.0	3.071	1.599	
14:	31.0	42.0	2.999	1.738	
15:	33.0	41.0	2.928	1.981	
16:	34.0	40.0	2.857	2.120	
17:	35.0	39.0	2.785	2.260	
18:	36.0	39.5	2.821	2.346	
19:	37.0	40.0	2.857	2.432	
20:	38.0	39.0	2.785	2.571	
21:	39.0	38.5	2.749	2.693	
22:	40.0	38.0	2.714	2.815	

23:	41.0	39.5	2.749	2.901
24:	43.0	39.0	2.785	3.091
25:	45.0	38.5	2.749	3.317
26:	47.0	38.0	2.714	3.542
27:	49.0	38.0	2.714	3.646
28:	49.0	37.0	2.642	3.785
29:	52.0	36.0	2.571	3.925
30:	52.0	35.5	2.535	4.150
31:	54.0	36.0	2.571	4.341
32:	56.0	36.5	2.607	4.531
33:	58.0	37.0	2.642	4.721
34:	60.0	37.5	2.678	4.911
35:	62.0	38.0	2.714	5.101
36:	64.0	38.0	2.714	5.309
37:	65.0	39.0	2.785	5.482
38:	68.0	39.5	2.821	5.672
39:	70.0	40.0	2.857	5.862
40:	72.0	40.5	2.892	6.052
41:	75.0	41.0	2.928	6.347
42:	77.0	41.5	2.964	6.537
43:	80.0	42.0	2.999	6.831
44:	82.0	42.5	3.035	7.021
45:	84.0	42.5	3.035	7.229
46:	86.0	42.5	3.035	7.437
47:	88.0	42.5	3.035	7.645
48:	90.0	43.0	3.071	7.835
49:	92.0	43.5	3.107	8.025
50:	94.0	44.0	3.142	8.215
51:	96.0	44.5	3.178	8.406
52:	98.0	45.0	3.214	8.596
53:	99.0	45.0	3.214	8.700 EZ

APPARATUS 733
SAMPLE NO. OT 3
DATE 06/16/75
OPERATOR TUCKER

CONSTANTS

K1(IN./LB.) = 1.700E-05
K2 (LB./DIV.) = 200.0
K3 (IN./LB.) = 1.000E-03
K4 (IN./LB.) = 7.500E-07

RECORDED BEFORE RUN		RECORDED AFTER RUN	
TEMPERATURE (DEGREES C.)	25.0	D(SAT)	-5.0
PORE PRESSURE (PSI)	0	D(SCP)	0
CONFINING PRESSURE (K-BARS)	.30	D(RSCP)	85.0
ANISOTROPY	0	D(RSAT)	75.0
SAMPLE LENGTH (IN.)	.9605	L(FR)	-22.0
SAMPLE DIAMETER (IN.)	.4920	L(FR)	0

CALCULATED

V(0) (CU.IN.)	.1826	E(CP) (PERCENT)	.18
L(CP) (IN.)	.9588	E(PAT) (PERCENT)	8.43
L(F) (IN.)	.9458	E(PCP) (PERCENT)	8.87
V(CP) (CU.IN.)	.1816	E(FCP) (PERCENT)	.61
A(F) (SQ.IN.)	.1920	P(C) (K-BARS)	.30

NO.	D(I)	L(I)	STRESS (K-BARS)	STRAIN (%)	
1:	0	0	0	0	
2:	5.0	5.0	.435	.309	=A
3:	9.0	10.0	.724	.490	
4:	10.0	13.0	.940	.582	
5:	13.0	18.0	1.300	.718	
6:	15.0	21.0	1.514	.924	
7:	18.0	24.0	1.728	1.026	
8:	20.0	27.0	1.942	1.128	=B
9:	21.0	28.0	2.013	1.197	
10:	22.0	29.0	2.083	1.266	
11:	23.0	29.5	2.117	1.353	=F
12:	24.0	28.0	2.010	1.510	
13:	25.0	27.5	1.974	1.632	
14:	27.0	27.0	1.938	1.859	
15:	29.0	25.5	1.830	2.016	
16:	29.0	23.5	1.687	2.191	
17:	31.0	24.0	1.723	2.382	
18:	33.0	24.0	1.723	2.591	
19:	35.0	23.5	1.687	2.817	
20:	37.0	23.0	1.651	3.043	
21:	39.0	23.5	1.687	3.234	
22:	41.0	23.5	1.687	3.443	
23:	43.0	23.0	1.651	3.669	
24:	45.0	23.0	1.651	3.878	
25:	47.0	23.0	1.651	4.086	
26:	50.0	23.0	1.651	4.399	
27:	55.0	23.0	1.651	4.921	
28:	60.0	23.0	1.651	5.442	
29:	65.0	22.5	1.615	5.981	
30:	70.0	22.0	1.579	6.521	
31:	75.0	22.0	1.579	7.042	
32:	80.0	22.0	1.579	7.564	
33:	85.0	22.0	1.579	8.085	
34:	90.0	22.0	1.579	8.607	
35:	95.0	22.0	1.579	9.128	
36:	98.0	21.0	1.507	9.476	=Z

APPARATUS 733
SAMPLE NO. QT 4
DATE 06/16/75
OPERATOR TUCKER

CONSTANTS

K1(IN./LB.) = 1.700E-06
K2 (LB./DIV.) = 200.0
K3 (IN./LB.) = 1.000E-03
K4 (IN./LB.) = 7.500E-07

RECORDED BEFORE RUN		RECORDED AFTER RUN	
TEMPERATURE (DEGREES C.)	25.0	D(SAT)	-16.0
PORE PRESSURE (PSI)	0	D(SCP)	0
CONFINING PRESSURE (K-BARS)	1.34	D(RSCP)	111.0
ANISOTROPY	0	D(RSAT)	94.0
SAMPLE LENGTH (IN.)	.9665	L(FR0)	-97.0
SAMPLE DIAMETER (IN.)	.4920	L(FR)	0

CALCULATED

V(0) (CU.IN.)	.1837	E(CP) (PERCENT)	.15
L(CP) (IN.)	.9650	E(PAT) (PERCENT)	11.38
L(F) (IN.)	.9563	E(PCP) (PERCENT)	11.50
V(CP) (CU.IN.)	.1829	E(ECP) (PERCENT)	2.52
A(F) (SQ.IN.)	.1913	P(C) (K-BARS)	1.34

NO.	D(I)	L(I)	STRESS (K-BARS)	STRAIN (%)	
1:	0	0	0	0	
2:	2.0	4.0	.291	.066	=A
3:	5.0	9.0	.653	.211	
4:	8.0	13.0	.942	.371	=B
5:	11.0	18.0	1.302	.506	
6:	14.0	23.0	1.662	.640	
7:	16.0	27.0	1.950	.707	
8:	20.0	33.0	2.378	.910	=F
9:	23.0	37.0	2.666	1.080	
10:	24.0	39.0	2.810	1.113	
11:	25.0	39.5	2.846	1.199	
12:	26.0	40.0	2.882	1.285	
13:	27.0	39.0	2.810	1.424	
14:	28.0	37.0	2.666	1.598	
15:	29.0	37.5	2.702	1.684	
16:	30.0	38.0	2.738	1.770	
17:	31.0	38.5	2.774	1.856	
18:	32.0	39.0	2.810	1.942	
19:	33.0	38.5	2.774	2.063	
20:	34.0	38.0	2.738	2.184	
21:	35.0	37.5	2.702	2.306	
22:	35.0	38.0	2.738	2.392	
23:	38.0	38.5	2.774	2.581	
24:	39.0	39.0	2.810	2.667	
25:	40.0	39.0	2.810	2.771	
26:	41.0	38.0	2.738	2.910	
27:	42.0	37.0	2.666	3.049	
28:	43.0	37.0	2.666	3.152	
29:	45.0	38.0	2.738	3.324	
30:	47.0	39.0	2.810	3.496	
31:	49.0	39.5	2.846	3.686	
32:	51.0	39.0	2.810	3.911	
33:	52.0	38.5	2.774	4.032	
34:	53.0	39.0	2.810	4.118	
35:	55.0	40.0	2.882	4.290	
36:	57.0	41.0	2.954	4.462	
37:	59.0	42.0	3.026	4.634	
38:	61.0	42.5	3.062	4.824	
39:	63.0	41.5	2.990	5.066	
40:	65.0	41.5	2.990	5.273	
41:	69.0	42.0	3.026	5.567	
42:	71.0	43.0	3.098	5.842	
43:	74.0	44.0	3.171	6.116	
44:	77.0	45.0	3.243	6.393	
45:	81.0	46.0	3.315	6.773	
46:	85.0	47.5	3.423	7.238	
47:	91.0	49.0	3.531	7.703	
48:	96.0	51.5	3.711	8.133	
49:	101.0	53.0	3.819	8.599	
50:	106.0	54.5	3.927	9.064	
51:	111.0	56.0	4.035	9.529	
52:	115.0	57.0	4.107	10.012	
53:	121.0	58.0	4.179	10.495	
54:	126.0	59.0	4.251	10.978	
55:	131.0	60.0	4.323	11.461	
56:	136.0	60.5	4.359	11.961	
57:	141.0	61.0	4.395	12.462	
58:	146.0	61.5	4.432	12.962	
59:	151.0	61.5	4.432	13.480	
60:	156.0	61.5	4.432	13.998	
61:	157.0	61.0	4.395	14.119	=Z

APPARATUS 733
SAMPLE NO. QT 5
DATE 06/16/75
OPERATOR TUCKER

CONSTANTS

K1(IN./LB.) = 1.700E-06
K2 (LB./DIV.) = 200.0
K3 (IN./LB.) = 1.000E-03
K4 (IN./LB.) = 7.500E-07

RECORDED BEFORE RUN		RECORDED AFTER RUN	
TEMPERATURE (DEGREES C.)	25.0	D(SAT)	-20.0
PORE PRESSURE (PSI)	0	D(SCP)	0
CONFINING PRESSURE (K-BARS)	1.67	D(RSCP)	90.0
ANISOTROPY	0	D(RSAT)	62.0
SAMPLE LENGTH (IN.)	.9610	L(FRO)	-121.0
SAMPLE DIAMETER (IN.)	.4920	L(FR)	0

CALCULATED

V(S) (CU.IN.)	.1927	E(CP) (PERCENT)	.19
L(CP) (IN.)	.9591	E(PAT) (PERCENT)	9.53
L(F) (IN.)	.9469	E(PCP) (PERCENT)	9.38
V(CP) (CU.IN.)	.1916	E(ECP) (PERCENT)	2.21
A(F) (SQ.IN.)	.1918	P(C) (K-BARS)	1.67

NO.	D(I)	L(I)	STRESS (K-BARS)	STRAIN (%)	
1:	0	0	0	0	
2:	5.0	9.0	.654	.202	EA
3:	9.0	12.0	.869	.513	
4:	14.0	24.0	1.736	.609	
5:	17.0	29.0	2.095	.744	
6:	20.0	34.0	2.453	.880	EB
7:	22.0	37.0	2.666	.982	
8:	23.0	39.0	2.810	1.016	
9:	24.0	40.0	2.890	1.094	
10:	25.0	40.5	2.913	1.171	
11:	26.0	40.5	2.910	1.275	EF
12:	27.0	39.5	2.838	1.415	
13:	29.0	37.5	2.694	1.694	
14:	31.0	36.0	2.587	1.956	
15:	32.0	35.5	2.551	2.078	
16:	33.0	35.0	2.515	2.200	
17:	34.0	35.5	2.551	2.286	
18:	36.0	36.0	2.587	2.477	
19:	38.0	37.0	2.659	2.650	
20:	39.0	37.5	2.694	2.737	
21:	40.0	37.5	2.694	2.841	
22:	41.0	37.0	2.659	2.963	
23:	42.0	36.5	2.623	3.085	
24:	44.0	37.0	2.659	3.276	
25:	46.0	38.0	2.730	3.449	
26:	48.0	39.0	2.802	3.622	
27:	50.0	39.5	2.838	3.813	
28:	52.0	40.0	2.874	4.004	
29:	53.0	40.5	2.910	4.090	
30:	54.0	40.5	2.910	4.194	
31:	55.0	40.5	2.910	4.299	
32:	56.0	39.0	2.802	4.456	
33:	57.0	38.5	2.766	4.578	
34:	58.0	39.0	2.802	4.665	
35:	59.0	39.5	2.838	4.751	
36:	61.0	41.0	2.946	4.906	
37:	64.0	43.0	3.090	5.148	
38:	69.0	46.0	3.305	5.563	
39:	74.0	48.0	3.449	6.014	

40:	79.0	50.0	3.593	6.464
41:	84.0	52.5	3.772	6.897
42:	89.0	55.0	3.952	7.329
43:	94.0	57.5	4.036	7.796
44:	99.0	59.0	4.239	8.230
45:	104.0	61.0	4.383	8.681
46:	109.0	62.5	4.491	9.149
47:	114.0	64.0	4.599	9.617
48:	119.0	66.0	4.742	10.067
49:	124.0	67.5	4.850	10.535
50:	129.0	69.0	4.958	11.003
51:	134.0	70.5	5.066	11.472
52:	135.0	70.0	5.030	11.594